U.S.A. **92,** 910–914
22. Takamura-Enya, T., Ishikawa, S., Mochizuki, M., and Wakabayashi, K. (2006) *Chem. Res. Toxicol.* **19,** 770–778
23. Masuda, Y., Suzuki, M., Piao J., Gu, Y., Tsurimoto, T., and Kamiya, K. (2007) *Nucleic Acids Res.* **35,** 6904–6916
24. Masutani, C., Kusumoto, R., Iwai, S., and Hanaoka, F. (2000) *EMBO J.* **19,** 3100–3109
25. Niimi, N., Sassa, A., Katafuchi, A., Grúz, P., Fujimoto, H., Bonala, R. R., Johnson, F., Ohta, T., and Nohmi, T. (2009) *Biochemistry* **48,** 4239–10234246
26. Masuda, Y., and Kamiya, K. (2002) *FEBS Lett.* **520,** 88–92
27. Masuda, Y., Ohmae, M., Masuda, K., and Kamiya, K. (2003) *J. Biol. Chem.* **278,** 12356–12360
28. Sambrook, J., Fritsch, E. F., and Maniatis, T. (1989) *Molecular Cloning: A Laboratory Manual*, 2nd Ed., Cold Spring Harbor Laboratory, Cold Spring Harbor, NY
29. Fukuda, H., and Ohtsubo, E. (1997) *Genes Cells* **2,** 735–751
30. Fukuda, H., Katahira, M., Tsuchiya, N., Enokizono, Y., Sugimura, T., Nagao, M., and Nakagama, H. (2002) *Proc. Natl. Acad. Sci. U.S.A.* **99,** 12685–12690
31. Sugiyama, H., and Saito, I. (1996) *J. Am. Chem. Soc.* **118,** 7063–7068
32. Mozzherin, D. J., Shibutani, S., Tan, C. K., Downey, K. M., and Fisher, P. A. (1997) *Proc. Natl. Acad. Sci. U.S.A.* **94,** 6126–6231
33. Sugimura, T., and Adamson, R. H. (2000) in *Food Borne Carcinogens: Heterocyclic Amines* (Nagao, M., and Sugimura, T., eds) pp. 1–4, John Wiley & Sons Ltd., Chichester, UK
34. Choi, J. Y., Stover, J. S., Angel, K. C., Chowdhury, G., Rizzo, C. J., and Guengerich, F. P. (2006) *J. Biol. Chem.* **281,** 25297–25306
35. Nakagama, H., Ochiai, M., Ubagai, T., Tajima, R., Fujiwara, K., Sugimura, T., and Nagao, M. (2002) *Mutat. Res.* **506–507,** 137–144
36. Nagao, M. (1999) *Mutat. Res.* **431,** 3–12
37. Nagao, M., Ushijima, T., Toyota, M., Inoue, R., and Sugimura, T. (1997) *Mutat. Res.* **376,** 161–167
38. Dashwood, R. H., Suzui, M., Nakagama, H., Sugimura, T., and Nagao, M. (1998) *Cancer Res.* **58,** 1127–1129
39. Prakash, S., Johnson, R. E., and Prakash, L. (2005) *Annu. Rev. Biochem.* **74,** 317–353
40. Nelson, J. R., Lawrence, C. W., and Hinkle, D. C. (1996) *Nature* **382,** 729–731
41. Haracska, L., Prakash, S., and Prakash, L. (2002) *J. Biol. Chem.* **277,** 15546–15551
42. Johnson, R. E., Washington, M. T., Haracska, L., Prakash, S., and Prakash, L. (2000) *Nature* **406,** 1015–1019
43. Haracska, L., Unk, I., Johnson, R. E., Johansson, E., Burgers, P. M., Prakash, S., and Prakash, L. (2001) *Genes Dev.* **15,** 945–954
44. Kim, S. R., Maenhaut-Michel, G., Yamada, M., Yamamoto, Y., Matsui, K., Sofuni, T., Nohmi, T., and Ohmori, H. (1997) *Proc. Natl. Acad. Sci. U.S.A.* **94,** 13792–13797
45. Kobayashi, S., Valentine, M. R., Pham, P., O'Donnell, M., and Goodman, M. F. (2002) *J. Biol. Chem.* **277,** 34198–34207
46. Ogi, T., Kato, T., Jr., Kato, T., and Ohmori, H. (1999) *Genes Cells* **4,** 607–618
47. Ohashi, E., Bebenek, K., Matsuda, T., Feaver, W. J., Gerlach, V. L., Friedberg, E. C., Ohmori, H., and Kunkel, T. A. (2000) *J. Biol. Chem.* **275,** 39678–39684
48. Ling, H., Boudsocq, F., Woodgate, R., and Yang, W. (2001) *Cell* **107,** 91–102

Published online 12 March 2009

Nucleic Acids Research, 2009, Vol. 37, No. 9 2841–2853
doi:10.1093/nar/gkp138

Protein hnRNP A1 and its derivative Up1 unfold quadruplex DNA in the human *KRAS* promoter: implications for transcription

Manikandan Paramasivam[1], Alexandro Membrino[1], Susanna Cogoi[1], Hirokazu Fukuda[2], Hitoshi Nakagama[2,] and Luigi E. Xodo[1,*]

[1]Department of Biomedical Science and Technology, School of Medicine, P.le Kolbe 4, 33100 Udine, Italy and [2]Biochemistry Division, National Cancer Center Research Institute, 1-1, Tsukiji 5, Chuo-ku, Tokyo 104-0045, Japan

Received December 9, 2008; Revised and Accepted February 18, 2009

ABSTRACT

The promoter of the human *KRAS* proto-oncogene contains a structurally polymorphic nuclease hypersensitive element (NHE) whose purine strand forms a parallel G-quadruplex structure (called 32R). In a previous work we reported that quadruplex 32R is recognized by three nuclear proteins: PARP-1, Ku70 and hnRNP A1. In this study we describe the interaction of recombinant hnRNP A1 (A1) and its derivative Up1 with the *KRAS* G-quadruplex. Mobility-shift experiments show that A1/Up1 binds specifically, and also with a high affinity, to quadruplex 32R, while CD demonstrates that the proteins strongly reduce the intensity of the 260 nm-ellipticity—the hallmark for parallel G4-DNA—and unfold the G-quadruplex. Fluorescence resonance energy transfer melting experiments reveal that A1/Up1 completely abrogates the cooperative quadruplex-to-ssDNA transition that characterizes the *KRAS* quadruplex and facilitates the association between quadruplex 32R and its complementary polypyrimidine strand. When quadruplex 32R is stabilized by TMPyP4, A1/Up1 brings about only a partial destabilization of the G4-DNA structure. The possible role played by hnRNP A1 in the mechanism of *KRAS* transcription is discussed.

INTRODUCTION

The mammalian *KRAS* gene encodes for a guanine nucleotide-binding protein of 21 kDa that activates several cellular pathways controlling important events such as proliferation, differentiation and signalling (1). The Ras proteins behave as a molecular switch cycling between inactive GDP-bound and active GTP-bound states. The state of nucleotide occupancy is regulated by specific proteins named guanine nucleotides exchange factors (GEFs) and GTPases activating proteins (GAPs) (1,2). The *RAS* genes are frequently mutated in solid and haematological neoplasias with single point mutations at exons 12, 13 and 61 (3,4). The most common mutated *RAS* gene in solid tumours is *KRAS*, with a 90% incidence in pancreatic adenocarcinomas (5,6). As the mutated Kras protein has a defective GTPase activity, it is not inactivated by GAPs (7). It remains locked into the GTP-bound active state which continuously transmits to the nucleus mitotic signals that contribute to the neoplastic phenotypes in cancer cells (8–10). As pancreatic adenocarcinomas are refractory to conventional treatments, the discovery of new drugs capable to sensitize tumour cells to chemotherapy is being pursued in many laboratories. In our laboratory, we focused on *KRAS* and in order to design anti-*KRAS* drugs we investigated how the transcription of this proto-oncogene is controlled. Previous studies have shown that a nuclease hypersensitive element (NHE), located in the *KRAS* promoter upstream of the transcription start between −327 and −296, is responsible for most of the transcription activity (11). Earlier we reported that the purine strand of NHE is structurally polymorphic, as its tract of sequence recognized by nuclear proteins is able to fold into stable G-quadruplex structures (12,13). Using the purine strand of NHE (called 32R) in quadruplex conformation as a bait, we pulled down from a pancreatic nuclear extract three proteins with affinity for the *KRAS* quadruplex. By SDS–PAGE and mass spectrometry, we identified these proteins as poly[ADP-ribose] polymerase 1 (PARP-1), ATP-dependent DNA helicase 2, subunit 1 (Ku70) and heterogeneous ribonucleoprotein A1 (hnRNP A1) (13). Protein hnRNP A1 (from now on A1) is a member of the heterogeneous ribonucleoprotein family, which is highly abundant in the nucleus of actively

*To whom correspondence should be addressed. Tel: +39 432 494395; Fax: +39 432 494301; Email: luigi.xodo@uniud.it

The authors wish it to be known that, in their opinion, the first two authors should be regarded as joint First Authors.

growing mammalian cells (14,15). All members of the hnRNP family are characterized by two highly conserved RNA recognition motifs (RRMs) at the *N*-terminus and by a glycine-rich domain at the *C*-terminus (16,17). Although a recent structure of a co-crystal of Up1 (a proteolitic portion of A1 retaining binding activity) bound to the telomeric repeat $(TTAGGG)_2$ suggests that both RRMs interact with DNA (18), it has been reported that only one motif (RRM1) is sufficient for strong and specific binding to single-stranded telomeric DNA (19) and that its sub-element RNP11 mediates destabilization of quadruplex $(CGG)_n$ (20). Proteins hnRNP play various roles in mRNA metabolism (14,15) and in the biogenesis of telomeres (21). As protein A1 (and its derivative Up1) was reported to have a telomere-lengthening effect in erytroleukemia cells (21,22), it is suspected to function as an auxiliary factor of the telomerase holoenzyme (23). Considering that the 3′ G-rich repeats of the telomeres are folded in stable G-quadruplex structures, it has been hypothesized that A1 stimulates telomere elongation by disrupting high-order structures formed by the telomere repeats. Indeed, Up1 was reported to destabilize the bimolecular quadruplex formed by human telomere repeats d(TTAGGGTTAGGG), $d(TTAGGG)_4$ and the intramolecular quadruplex of $d(GGCAG)_5$ (23–25).

Since we discovered that A1 is associated to the *KRAS* promoter, in this study we have investigated the interaction between recombinant A1/Up1 and the *KRAS* G-quadruplex. Electrophoretic mobility shift assay (EMSA) showed that A1/Up1 binds to the *KRAS* quadruplex with high affinity and specificity, while CD and fluorescence resonance energy transfer (FRET) experiments revealed that A1/Up1 destabilizes this non B-DNA structure of the *KRAS* promoter. The results of our study support a transcription mechanism in which A1 should function as a G-quadruplex destabilizing protein, as it seems to occur in the G-rich 3′ overhang strand of the telomeres (23). In conclusion, this study sheds some light on the mechanism of *KRAS* transcription regulation and may be useful for the rationale design of anticancer drugs specific for oncogenic *KRAS*.

MATERIALS AND METHODS

DNA and proteins hnRNP A1/Up1

The oligonucleotides used in this study (Table 1) were obtained from MWG (Germany) and Microsynth (Switzerland). They have been purified by 20% PAGE (acrylamide: bisacrylamide, 19:1) in TBE, under denaturing conditions (7 M urea, 55°C). The bands were excised from the gel and eluted in water. The DNA solutions were filtered (Ultrafree-DA, Millipore) and precipitated. DNA concentration was determined from the absorbance at 260 nm of the oligonucleotides diluted in milli Q water, using as extinction coefficients 7500, 8500, 15 000 and 12 500 $M^{-1}cm^{-1}$ for C, T, A and G, respectively. Dual-labelled F-32R-T (5′ end with FAM, 3′ end with TAMRA) were HPLC-purified.

Recombinant proteins Up1 and A1 tagged to GST were expressed in *Escherichia coli* BL21 using plasmids pGEX-Up1 and pGEX-hnRNP A1. After transformation, the bacteria were grown for 2 h at 37°C with 50 μg/ml ampicillin to an A_{600} of 0.5–2.0 prior to induction with IPTG (100 μM final concentration). Cells were allowed to grow for 7 h before harvesting. The cells were centrifuged at 5000 r.p.m., 4°C. After centrifugation the supernatant was removed carefully and the cells washed twice with PBS. The pellet was re-suspended in a solution of PBS with PMSF 100 mM and DTT 1 M. The bacteria were lysed by sonication, added with Triton X-100 (1% final concentration) and incubated for 30 min on a shaker at room temperature. The lysate was then centrifuged for 10 min at 4°C at 10 000 r.p.m. Glutathione Sepharose 4B (GE Healthcare) (50% slurry in PBS) was added to the supernatant and incubated for 30 min at 4°C on a shaker. The mix was centrifuged for 5 min at 500 g and the pellet was washed 5 times in PBS and eluted with elution buffer containing 20 mM NaCl, 20 mM reduced glutathione, 200 mM Tris–HCl, pH 9.5 for A1 elution and pH 7.5 for Up1 elution. Alternatively, to remove the GST tag, the mix was centrifuged for 5 min at 500*g*, washed with PreScission Cleavage buffer (GE Healthcare) and centrifuged 5 min at 500*g*. The pellet was incubated for 4 h at 4°C with PreScission protease to cleave the GST tag from the purified proteins. After PreScission cleavage, the A1 or Up1 moieties were detached from GST which remained bound to the Gluthatione Sephadex beads. The reaction mixtures were centrifuged for 5 min at 500*g*, 4°C, and the untagged proteins collected from the supernatant. Finally, the purification of tagged and untagged Up1 and A1 proteins were checked by SDS–PAGE.

CD and fluorescence experiments

CD spectra have been obtained with a JASCO J-600 spectropolarimeter equipped with a thermostatted cell holder. CD experiments were carried out with oligonucleotides (3 μM) in 50 mM Tris–HCl, pH 7.4, 100 mM KCl. Spectra were recorded in 0.5 cm quartz cuvette. A thermometer inserted in the cuvette holder allowed a precise measurement of the sample temperature. The spectra were calculated with J-700 Standard Analysis software (Japan Spectroscopic Co., Ltd) and are reported as ellipticity (mdeg) versus wavelength (nm). Each spectrum was recorded three times, smoothed and subtracted to the baseline.

Fluorescence measurements were carried out with a Microplate Spectrofluorometer System (Molecular Devices) using a 96-well black plate, in which each well contained 50 μl of 200 nM dual-labelled F-32R-T in 50 mM Tris–HCl, pH 7.4 and KCl as specified in the figure captions. Before adding the protein, the samples were incubated for 24 h at room temperature in the specified buffer. The protein (Up1, A1 or BSA) was added 30 min before fluorescence analysis. The emission spectra were obtained by setting the excitation wavelength at 475 nm, the cut-off at 515 nm and recording the emission from 500 to 650 nm. Upon addition of KCl, F-32R-T assumes a folded quadruplex conformation and FRET is expected between the 5′ and 3′ fluorophores. The emission

intensity of the donor (FAM) decreases while the intensity of the acceptor increases, correspondingly, as K^+ is added to the sample solution. The energy transfer from the donor to the acceptor and vice versa can be empirically represented by the parameter P:

$$P = \frac{I_D}{(I_D + I_A)}$$

where I_D and I_A are the intensities of the donor and acceptor (26,27). Fluorescence melting experiments were performed on a real-time PCR machine (iQ5, BioRad), using a 96-well plate filled with 50 µl solutions of dual-labelled F-32R-T. The protocol used for the melting experiments is the following: (i) equilibration step of 5 min at low temperature (15°C); (ii) stepwise increase of the temperature of 1°C per min for 76 cycles to reach 95°C. All samples in the wells were melted in 76 min.

Kinetic experiments were carried out using the iQ5 real-time machine. Oligonucleotide F-32R-T (200 nM) in 100 mM KCl, i.e. in the quadruplex conformation, was mixed with the complementary 32Y strand and the increase at 525 nm of the fluorescence was measured as a function of time. The experiment was also performed adding to F-32R-T a mixture containing 32Y (8-fold) and Up1 (400 nM). The increase of fluorescence $\Delta F = F - F_0$, where F_0 and F is the fluorescence at 525 nm (FAM) at $t = 0$ and at any time t, was best-fitted to a single or double-exponential curve. The half-life of the reaction is given by $t_{1/2} = 0.693/k$.

EMSA

Oligonucleotides 32R, *HRAS-1*, *HRAS-2*, *CMYC*, *CKIT*, *VEGF*, 32Y, Gmut1 and Gmut2 were end-labelled with [γ-^{33}P]ATP and T4 polynucleotide kinase. Duplex dsNHE was prepared annealing (10 min at 95°C, overnight at room temperature) a mixture containing equimolar amounts of radiolabelled 32R and complementary 32Y in 50 mM Tris–HCl, pH 7.4, 100 mM NaCl. Before EMSA, the quadruplex-forming oligonucleotides were allowed to form their structure in 50 mM Tris–HCl, pH 7.4, 100 mM KCl, 37°C (overnight incubation). Radiolabelled oligonucleotides (35 nM) were treated for 30 min at room temperature with different amounts of A1/Up1, (r ([protein]/[oligonucleotide]) ratios are specified in Figure 3) in 20 mM Tris–HCl, pH 8, 30 mM KCl, 1.5 mM $MgCl_2$, 1 mM DTT, 8% glycerol, 1% Phosphatase Inhibitor Coktail I (Sigma, Milan, Italy), 5 mM NaF, 1 mM Na_3VO_4, 2.5 ng/ml poly [dI-dC]. After incubation, the reaction mixtures were loaded in 8% TBE (1×) polyacrylamide gel, thermostatted at 16°C. After running the gel was dried and exposed to autoradiography (G E Healthcare, Milan) for 24–36 h at −80°C.

Polymerase-stop assay

A linear DNA fragment of 87 nt, containing the G-rich element of NHE, was used as a template for Taq polymerase primer-extension reactions. This DNA sequence was purified by PAGE. The template (100 nM) was mixed with the labelled primer (50 nM) in 100 mM KCl, Taq buffer 1× and overnight incubated at 50°C. The primer extension reactions were carried out for 1 h, by adding 10 mM DTT, 100 µM dATP, dGTP, dTTP, dCTP and 3.75 U of Taq polymerase (Euro Taq, Euroclone, Milan). The reactions were stopped by adding an equal volume of stop buffer (95% formamide, 10 mM EDTA, 10 mM NaOH, 0.1% xylene cyanol, 0.1% bromophenol blue). The products were separated on a 15% polyacrylamide sequencing gel prepared in TBE, 8 M urea. The gel was dried and exposed to autoradiography. Standard dideoxy sequencing reactions were performed to detect the points in which DNA polymerase I was arrested.

RESULTS

We previously demonstrated that the G-rich strand of NHE can form G-quadruplex structures (13,28). By means of CD and DMS-footprinting experiments we found that the G-tract called 32R forms a parallel G-quadruplex characterized by three G-tetrads (T_m of 70°C in 100 mM KCl) (Figure 1). Pull-down assays with a pancreatic nuclear extract combined to mass spectrometry showed that quadruplex 32R binds to three proteins: PARP-1 (116 kDa), Ku70 (72 kDa) and A1 (34 kDa) (13). Since A1 is involved in the biogenesis of the telomeres as a G4-DNA destabilizing protein (23) and is able to disrupt the secondary structures of the hypervariable minisatellite sequence d(GGCAG)$_5$ (24), we asked whether A1/Up1 can have a similar functional role in the human *KRAS* promoter. To address this question, recombinant A1 and its derivative Up1 were expressed in *Escherichia coli* as proteins fused to GST and purified by affinity chromatography with glutathione sepharose 4B. The GST moiety was removed with a pre-scission protease and recombinant tagged and untagged proteins were obtained with a high purity level (Figure 2). Up1 is a proteolitic fragment (195 aa) of A1 (319 aa) that retains the two RNA-recognition motifs (RRMs) responsible for binding to nucleic acids (18,22).

The interaction between A1/Up1 and a variety of DNA substrates, some of which were structured in G4-DNA and some not, was analysed by EMSA. ^{33}P-labelled 32R (35 nM) was first incubated for 24 h in 100 mM KCl to allow quadruplex formation, then incubated for 30 min with increasing amounts of Up1 or A1: r ([protein]/[32R]) = 0, 0.5, 1, 2, 5, 10, 20, 50, 100. As preliminary experiments showed that GST-tagged and untagged proteins behave in the same way, we performed EMSA with the tagged proteins. Figure 3a and b shows that quadruplex 32R forms with A1/Up1 a DNA–protein complex that, being detected even at $r = 0.5$, should have a 1:1 stoichiometry. In addition, for $r > 20$, another slow-migrating DNA–protein complex appears in the gel, most likely due to a 1:2 complex. When r was increased to 200 and the samples run in a longer gel, 32R migrated essentially as 1:2 complex (Figure 3c). The formation of two DNA–protein complexes by A1/Up1 is in keeping with the results of Zhang *et al.* (23) and the crystal structure of d(TTAGGG)$_2$ bound to Up1 (18). Since a tract of 12 nt functions as a minimum binding unit, 32R has

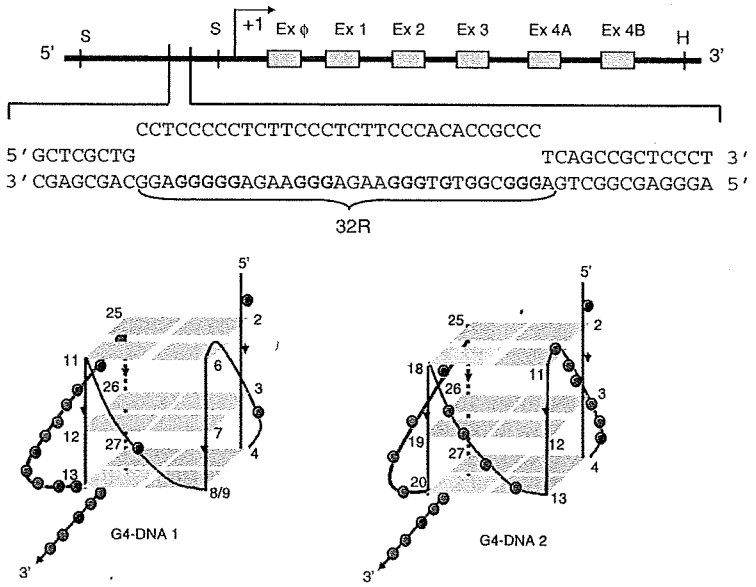

Figure 1. Sequence of the nuclease hypersensitive element (NHE) in the human *KRAS* promoter. The G-rich sequence 32R forms a G-quadruplex whose putative structure, consistent with CD and dimethyl sulfate footprinting, is G4-DNA1, which is characterized either by a flipped-out thymidine connecting G7 to G9 or a GGGT triad (13). The expected G4-DNA2 structure is not supported by dimethyl sulfate footprinting. The nucleotides of 32R (Table 1) are numbered from the 5'-end.

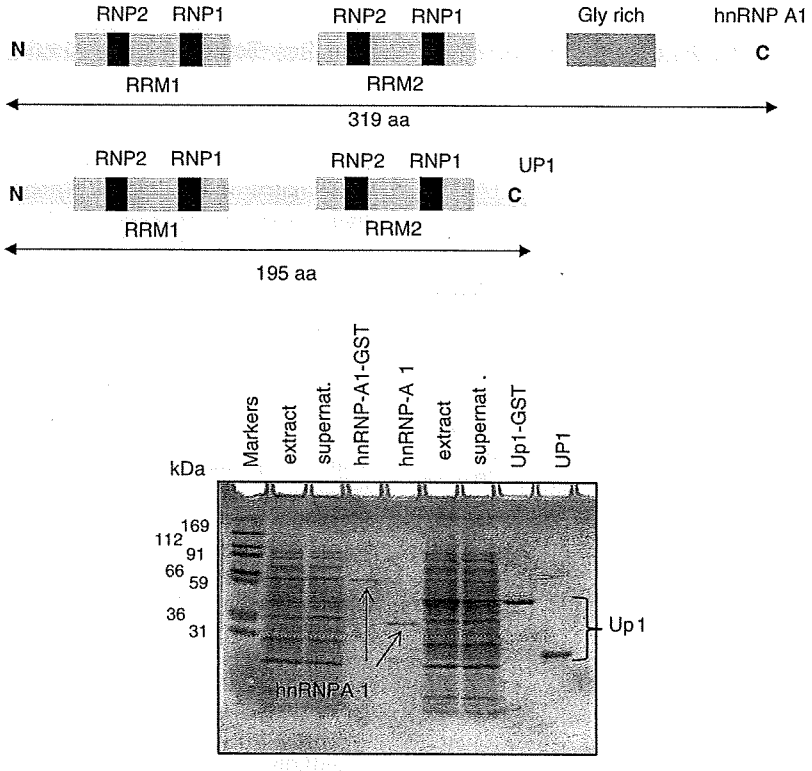

Figure 2. Schematic representations of proteins hnRNP A1 and Up1. The two RNA-recognition motifs (RRMs), that mediate ssDNA binding, contain each two conserved RNP2 and RNP1 submotifs. Up1 encompasses the amino-terminal two-third of the hnRNPA1 sequence. SDS PAGE of GST-tagged and untagged hnRNP A1 and Up1, after gluthatione sepharose 4B purification. Lane 1, protein markers; lane 2, total extract (hnRNP A1); lane 3, supernatant; lane 4, purified GST-tagged hnRNP A1; lane 5, purified untagged hnRNP A1; lane 6, total extract (Up1); lane 7, supernatant; lane 8, purified GST-tagged Up1; lane 9, purified untagged Up1.

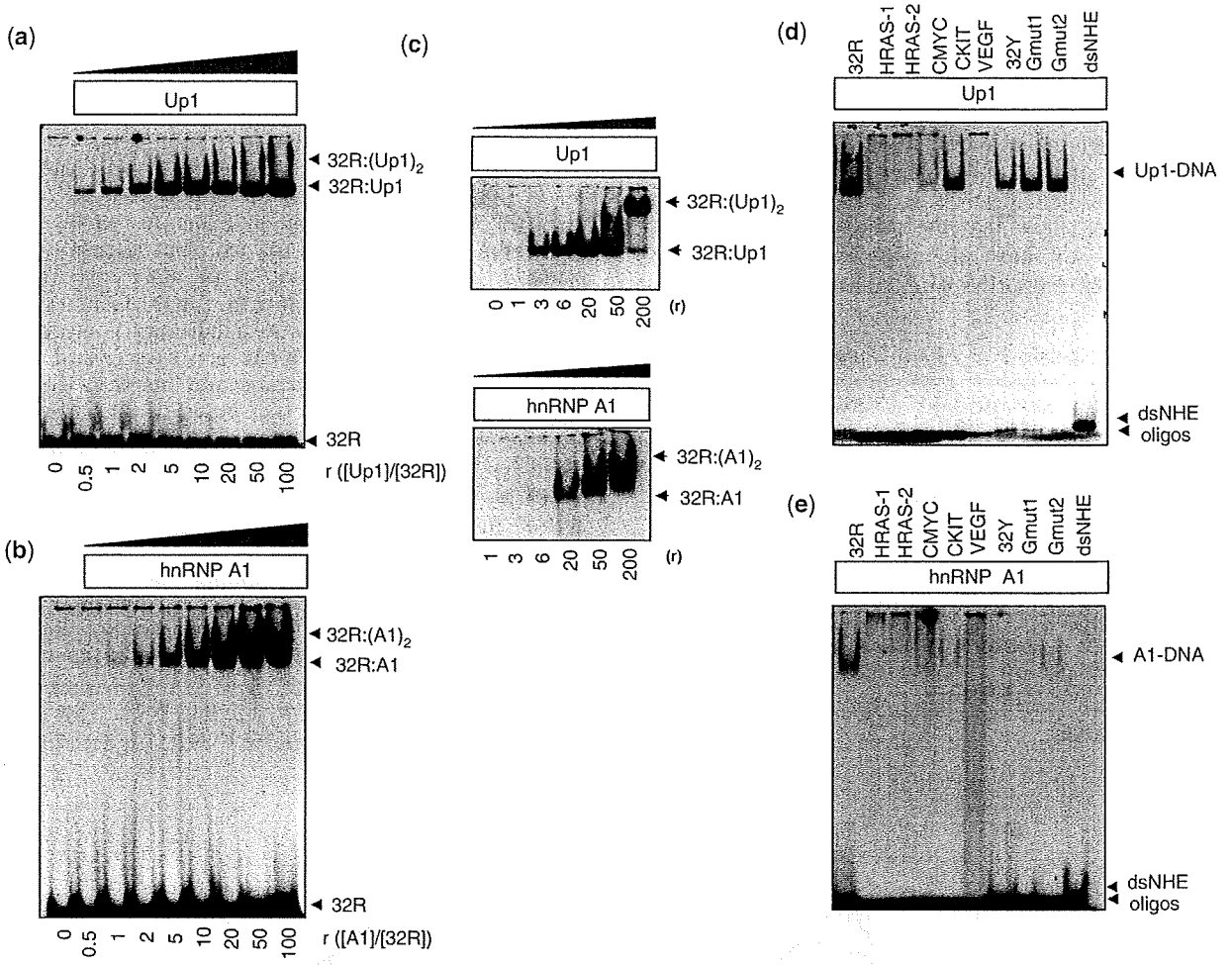

Figure 3. (**a**, **b**) EMSA of 35 nM ^{33}P-labelled quadruplex 32R after 30 min incubation with increasing amounts of Up1 or A1 at the specified r values, in 20 mM Tris–HCl, pH 8, 30 mM KCl, 1.5 mM $MgCl_2$, 1 mM DTT, 8% glycerol, 1% Phosphatase Inhibitor Coktail 1 (Sigma), 5 nM NaF, 1 mM Na_3VO_4, 2.5 ng/μl poly dI-dC, for 25°C. The analyses were carried out in 8% polyacrylamide gel (29:1) in TBE (1×) at 16°C. Before the EMSA, 32R was incubated overnight in 100 mM KCl to get it in the G-quadruplex conformation; (**c**) EMSA as in (a, b) but with r values up to 200; (**d**, **e**) EMSA of A1/Up1 mixed to various DNA substrates [G-quadruplexes 32R, *HRAS*-1, *HRAS*-2, *CMYC*, *CKIT*, *VEGF*, dsNHE (32R:32Y) and unstructured oligonucleotides Gmut1, Gmut2, 32Y]. PAGE carried out in 8% polyacrylamide gel (29:1) in TBE (1×) at 16°C.

potentially two binding sites, which can in principle form two DNA–protein complexes by binding one or two protein molecules. By quantifying the intensity of the electrophoretic bands, we roughly estimated that the dissociation constant K_d of the 1:1 complex is about 50 nM for Up1 and 200 nM for A1. We also tested the binding specificity of A1/Up1 for a variety of well known G-quadruplex structures obtained from *CMYC*, *CKIT*, *VEGF* and *HRAS* promoter sequences (29–32) (for *HRAS* quadruplexes, see Supplementary Data S1) (Figure 3d and e). The various DNA substrates have been ^{33}P-labelled and treated with an excess of protein ($r = 50$). It can be seen that A1 shows good specificity for the *KRAS* quadruplex, as it does not bind to the other quadruplex-forming sequences, unstructured oligonucleotides Gmut1, Gmut2, 32Y (the complementary polypyrimidinic NHE strand) and dsNHE (32R:32Y) (Table 1). Instead, protein Up1, besides quadruplex 32R, shows affinity also for the *CKIT* quadruplex and unstructured oligonucleotides.

To analyse the effect of A1/Up1 on the *KRAS* G-quadruplex, we could not employ electrophoresis because the mobility between an *intra*molecular quadruplex and its unfolded form is not very different. Therefore, we used spectroscopic techniques such as circular dichroism (CD) and FRET. Figure 4 shows that in 100 mM KCl, 32R is characterized by a CD signature typical of a parallel G-quadruplex: a strong and positive ellipticity at 260 nm and a weak and negative ellipticity at 240 nm (33). When quadruplex 32R is denatured by increasing the temperature, the positive 260 nm band is dramatically reduced and its spectrum becomes similar to that of unstructured oligonucleotides (data not shown). Thus, the structural transition from quadruplex-to-ssDNA is accompanied by a strong reduction of the 260 nm ellipticity. A similar transition was obtained by adding to

quadruplex 32R increasing amounts of A1/Up1 (r = 1, 2, 4, 6). It can be seen that the protein causes a progressive reduction of the 260 nm ellipticity, indicating that the G4-DNA structure is unfolded by the protein. As a control, we treated quadruplex 32R with an unrelated protein, the trypsinogen inhibitor, and found that the 260 nm ellipticity was not affected and remained constant at all protein concentrations used. The CD spectra of Up1 at increasing concentrations show that the protein between 240 and 320 nm does not have any negative band, but below 240 nm it shows a negative band typical of the polypeptide backbone. The CD data showing G-quadruplex unfolding are in keeping with those previously obtained with the telomeric TTAGGG repeat (24,25) and the hypervariable minisatellite sequence d(GGCAG)$_5$ treated with Up1 (24).

The unfolding of the human *KRAS* quadruplex by A1/Up1 was also investigated by FRET, using the quadruplex-forming sequences tagged at the 5′ and 3′ ends with FAM (donor) and TAMRA (acceptor) (34). By exciting F-32R-T at 475 nm, the emission intensity of the donor at 525 nm decreases while the emission intensity of the acceptor at 580 nm increases, as the KCl concentration is increased from 0 to 140 mM (Supplementary Data S2). F-32R-T folded in the G-quadruplex conformation (T_m = 75°C in 140 mM KCl) is characterized by a P-value of 0.52 (see 'Materials and methods' section). This P-value is higher than that observed for the quadruplex formed by the human telomeric repeat d(GGGTTAG GGTTAGGGTTAGGG) (26), because F-32R-T forms a parallel quadruplex where the two fluorophores are at opposite ends of the structure (13). When the G-quadruplex is destabilized by scaling down the KCl concentration to zero or by adding the complementary 32Y strand, that transforms the G-quadruplex into a B-DNA duplex where the donor and acceptor are separated by about 115 Å, the donor fluorescence significantly increases (for instance, from spectrum 2 to spectrum 1, Figure 5a) and the P-value becomes 0.75. This means that the unfolding of quadruplex F-32R-T is accompanied

Table 1. Oligonucleotides (5′ > 3′) used in this study

AGGGCGGTGTGGGAAGAGGGAAGAGGGGGAGG	32R
F-AGGGCGGTGTGGGAAGAGGGAAGAGGGGGAGG-T	F-32R-T
AGGGAGGGCGCTGGGAGGAGGG	*CKIT*
GGGCGGGCCGGGGGCGGGTCCCGGCGGGG	*VEGF*
TGGGGAGGGTGGGGAGGGTGGGGAAGG	*CMYC*
TCGGGTTGCGGGCGCAGGGCACGGGCG	*HRAS*-1
CGGGGCGGGGCGGGGGCGGGGGCG	*HRAS*-2
GCGGTGTGTGAAGAGTGAAGAGTGGGATGCAG	Gmut1
GCATTCTGATTACACGTATTACCTTCACTCCA	Gmut2
CCTCCCCCTCTTCCCTCTTCCCACACCGCCCT	32Y
GTACTACACTTGATA	primer
ACCTTGATGAATCCAGGGCGGTGTGGGAAGAG	template
GGAAGAGGGGGAGGAATCGCTACCGTTAAGCA	
TCGATCATATCAAGTGATAGTAC	

F: FAM; T: TAMRA.

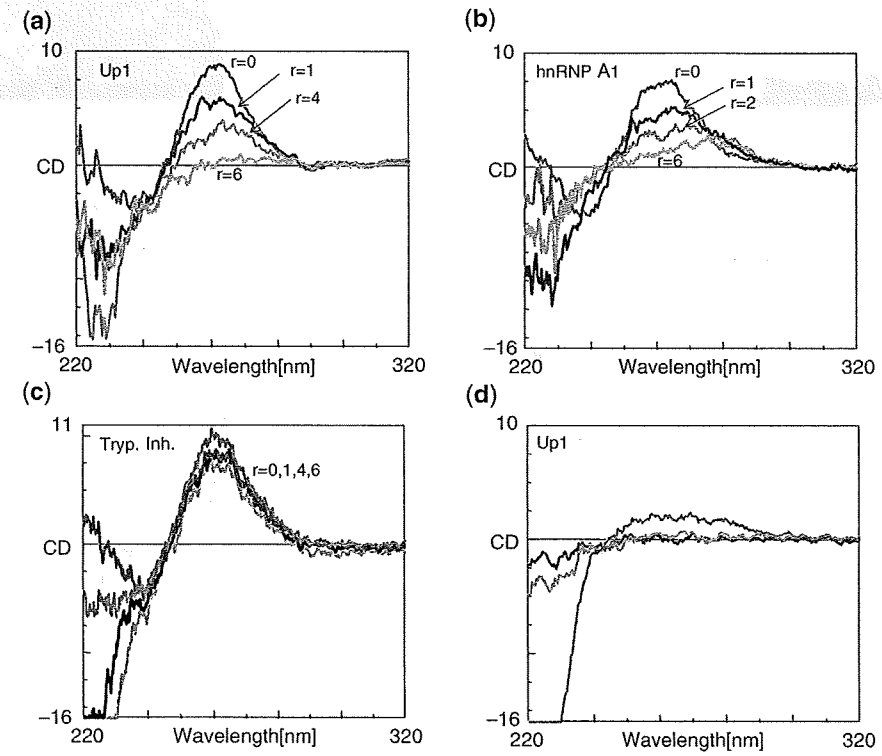

Figure 4. CD of 32R (2 μM) in 50 mM Tris pH 7.4, 100 mM KCl in the presence of increasing amounts of Up1 (r = 0, 1, 4, 6) (r = [protein]/[DNA]) (**a**); hnRNPA1 r = 0, 1, 4, 6, (**b**); trypsinogen inhibitor (TI) (r = 0, 1, 4, 6) (**c**). The CD of Up1 at three concentrations is reported (2, 4 and 8 μM) (**d**). Spectra have been recorded at room temperature with a path length cuvette of 0.5 cm. Ordinate reports ellipticity values in mdeg.

by a $\Delta P = 0.75 - 0.52 = 0.23$. We then asked if quadruplex F-32R-T is unfolded by A1/Up1. To choose at which ionic strength the FRET experiments in the presence of A1/Up1 should be performed, we measured the T_m of quadruplex F-32R-T in KCl and NaCl solutions (in 50, 100 and 140 mM KCl, T_m is 48, 70 and 75°C, respectively; in 100 mM NaCl, the T_m is 32°C). Figure 5a shows the effect on quadruplex F-32R-T in 50 mM KCl (T_m = 48°C,

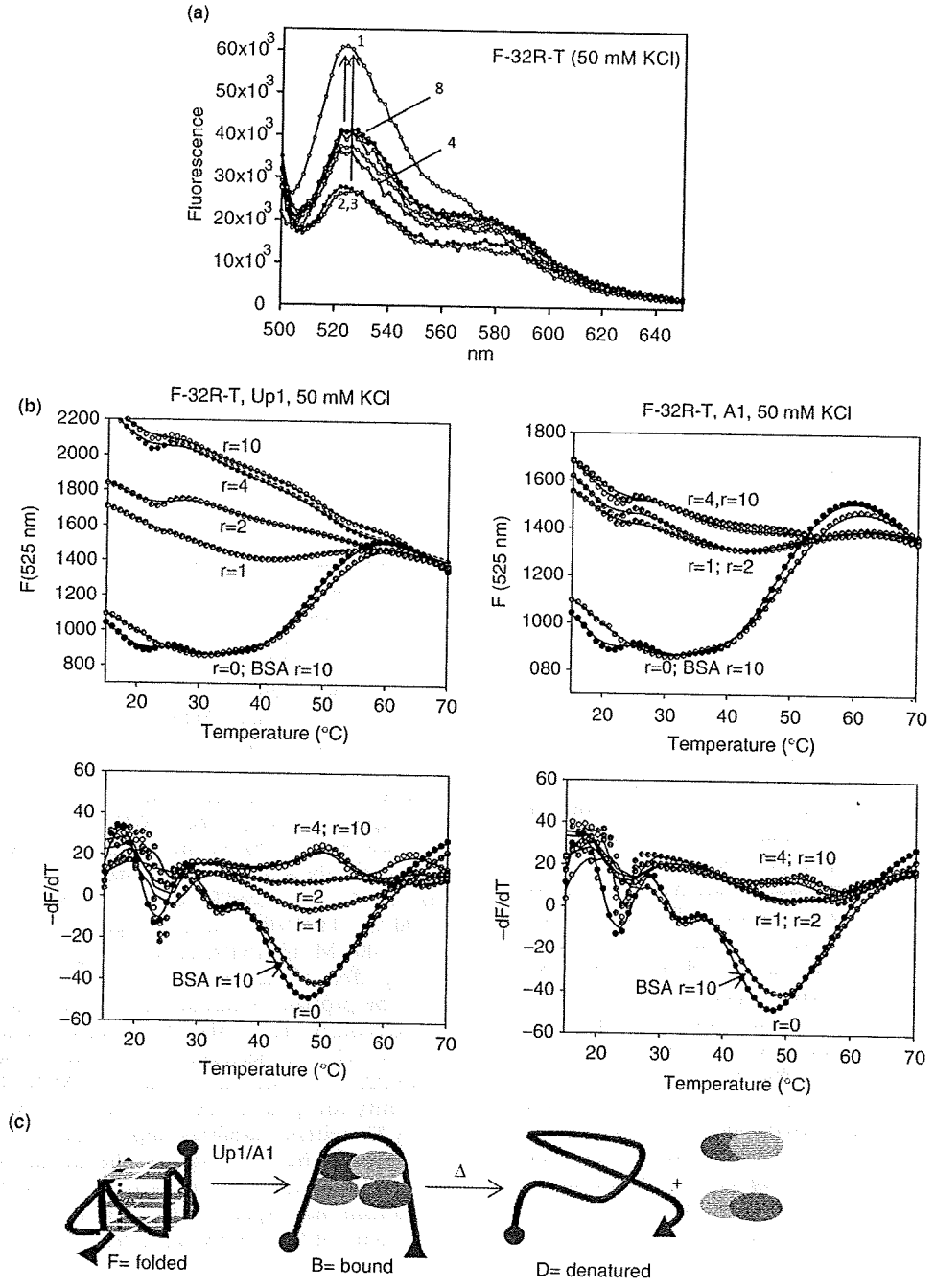

Figure 5. (a) Fluorescence spectra of 200 nM F-32R-T in water (spectrum 1) or 50 mM Tris-HCl, pH 7.4, 50 mM KCl in the absence (spectrum 2) or presence of BSA (r = 10, spectrum 3) or Up1 (r = 0.5, 1, 3, 6, 10, spectra 4–8); (b) row FRET-melting curves (F_{525} versus T) obtained with the iQ5 real-time PCR machine of quadruplex F-32R-T treated with A1/Up1 at various [protein]/[DNA] ratios, in 50 mM Tris pH 7.4, 50 mM KCl. As reference a melting curve of F-32R-T in the presence of BSA (r = 10) is reported. Bottom panels show the corresponding first derivative curves, dF_{525}/dT versus T. The G-quadruplex was incubated with the protein for 30 min prior to melting; (c) schematic representation of the U-shape structure of the DNA–protein complex between F-32R-T and Up1.

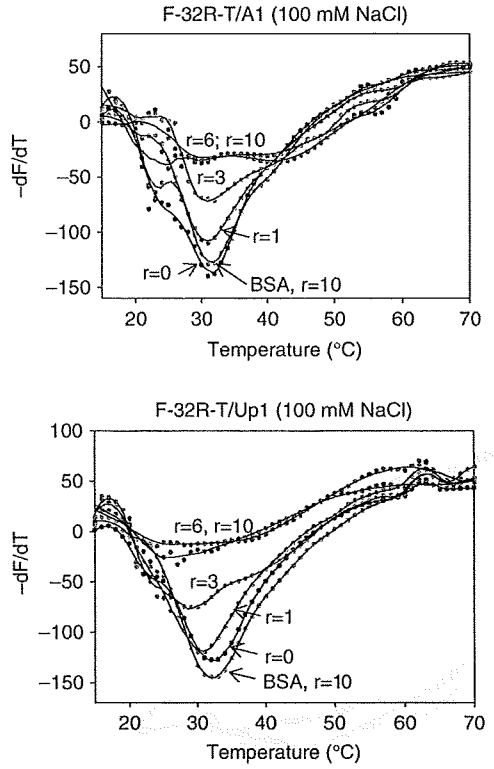

Figure 6. $-dF_{525}/dT$ versus T curves in 50 mM Tris pH 7.4, 100 mM NaCl of F-32R-T in the absence or presence of A1 (**a**), Up1(**b**), BSA at various [protein]/[DNA] ratios.

$P = 0.62$) of Up1 and A1 at $r = 1, 2, 3, 6, 10$. It can be seen that, compared to complementary 32Y, Up1 does not promote a significant increase of the donor emission, a behaviour that might suggest that Up1 has little effect on the quadruplex conformation [for instance the P-value is 0.62 at $r = 0$ (spectrum 2), 0.67 at $r = 10$ (spectrum 8), $\Delta P = 0.05$]. If we assume that $\Delta P = 0.23$ reflects total opening of the G-quadruplex, $\Delta P = 0.05$ suggests that F-32R-T bound to Up1 is partially opened (20%). Alternatively, it is possible that F-32R-T in the DNA–protein complex is completely opened but with the 5′ and 3′ ends brought close to one another so that FRET takes place. To gain insight into this possibility we performed melting experiments. We reasoned that in case the quadruplex is partially unfolded, its T_m would be lowered, whereas in case it is completely opened by A1/Up1, the quadruplex-to-ssDNA transition should be abrogated. Figure 5b shows typical melting curves for quadruplex F-32R-T in 50 mM KCl, obtained with a real-time PCR machine, after the DNA was incubated for 30 min with A1/Up1 ($r = 1, 2, 4, 10$) or BSA ($r = 10$) just before melting. It can be seen that an excess of BSA does not change the T_m of the G-quadruplex, as one expects with an unspecific protein which does not interact with DNA. In contrast, when quadruplex F-32R-T is incubated with A1/Up1, a strong change of the melting curves is observed. The cooperative transition relative to the denaturation of the G-quadruplex (T_m of 48°C) is completely abrogated and replaced with a broad and non-cooperative curve, which reflects the disruption of the DNA–protein complex. The abrogation of the quadruplex-to-ssDNA transition is clearly observed with both F versus T and $-dF/dT$ versus T curves. A similar behaviour has been reported for the UV-melting of the virus type 1 nucleocapsid protein bound to the quadruplex formed by d(GGGTTGGTGTG GTTGG) (35). In 100 mM NaCl, where quadruplex F-32R-T shows a cooperative transition with a T_m of 32°C, we also observed the abrogation of the cooperative transition by A1/Up1 (Figure 6). These data suggest that when F-32R-T is bound to A1/Up1, its secondary structure is completely disrupted and F-32R-T in the DNA–protein complex is in the single-stranded form. The fact that the opening of the quadruplex by Up1 is accompanied by a ΔP which is 20% of that observed with 32Y (0.05 against 0.23) can be rationalized on the basis of the crystal structure between Up1 and the telomeric repeat (T TAGGG)$_2$ (18). In the crystal, the two RRM elements within a Up1 molecule bind to two separate 12mer oligonucleotides, which are antiparallel and separated by an *inter*strand distance of 25–50 Å. Thus, we expect that F-32R-T bound to A1/Up1 adopts a U-shape with the two fluorophores close enough to promote energy transfer (18) (Figures 5c).

It is well known that the cationic porphyrin TMPyP4 stabilizes quadruplex DNA by stacking externally to the G-tetrads and interacting with the loop nucleotides (36). We therefore tested whether TMPyP4 reduces the quadruplex destabilizing action of A1/Up1. Quadruplex F-32R-T (200 nM) was incubated for 12 h in 50 mM KCl, in the presence of 200 and 600 nM TMPyP4. Figure 7a shows that TMPyP4 enhances the T_m of quadruplex F-32R-T from 48°C (curve 1) to 68 (curve 4) and 76°C (curve 5). The mixtures were treated for 30 min with 1 μM A1 ($r = 5$) and then melted. While A1 at $r = 5$ is able to completely disrupt the *KRAS* quadruplex in 50 mM KCl (see Figure 5b), in the presence of the porphyrin it promotes only a partial destabilization of the G-quadruplex: the T_m is reduced from 68°C to 58°C (in the presence of 200 nM TMPyP4, curve 2, Figure 7a) or from 76°C to 63°C (600 nM TMPyP4, curve 3, Figure 7a). So, the stabilizing effect of the porphyrin partially inhibits the capacity of the protein to unfold the G-quadruplex. To exclude the possibility that TMPyP4 directly interacts with and inhibits A1, we performed a control experiment with TMPyP2, the positional isomer of TMPyP4 showing little affinity for quadruplex DNA (Figure 7b). As expected, TMPyP2 neither stabilizes appreciably quadruplex 32R, nor impairs the unfolding of the quadruplex structure by A1. These experiments provide a possible molecular mechanism that explains how TMPyP4 is found to repress the activity of the *KRAS* promoter (12,13).

Krainer and co-workers (23) showed that A1/Up1 binds to the single-stranded and structured human telomeric repeat $(TTAGGG)_{n=2,4}$. They suggest that A1 is likely to function as an auxiliary factor of the telomerase holoenzyme and propose that the protein stimulates telomerase elongation through unwinding of the G-quadruplex structures formed during the

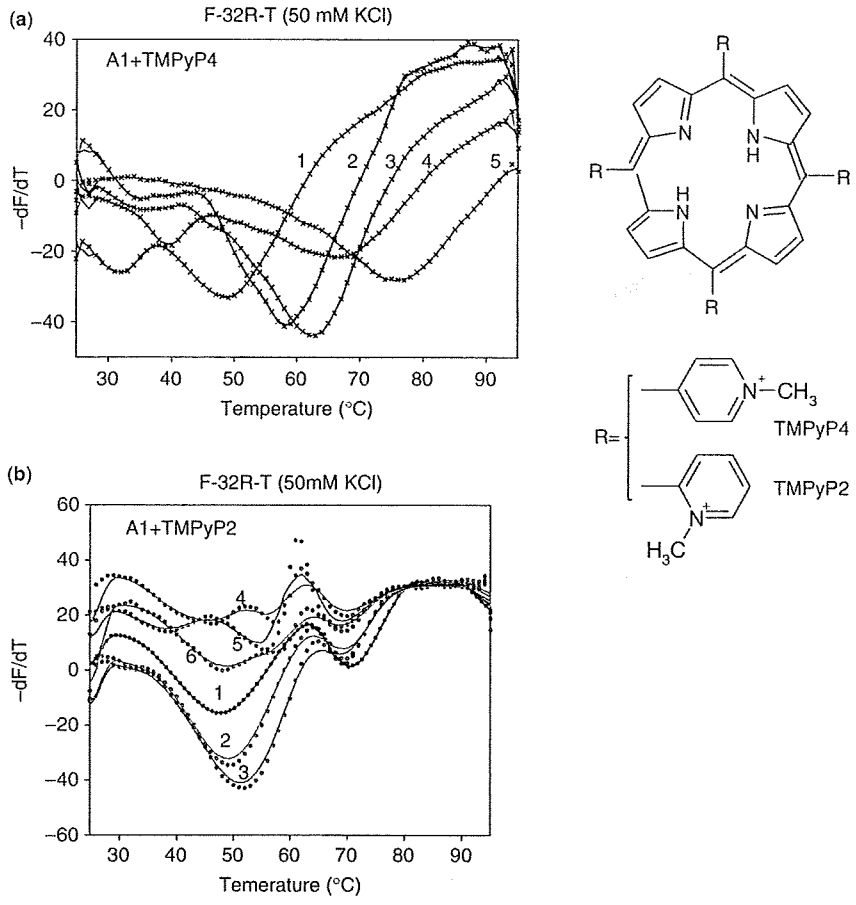

Figure 7. (a) $-dF_{525}/dT$ versus T melting curves of 200 nM F-32R-T in 50 mM Tris pH 7.4, 50 mM KCl (curve 1), in the presence of 200 nM (curve 4) or 600 nM (curve 5) porphyrin TMPyP4. Curves 2 and 3 show the melting curves obtained by F-32R-T treated with 200 nM TMPyP4 + A1 ($r = 5$) or 600 nM TMPyP4 + A1 ($r = 5$), respectively; (b) dF_{525}/dT versus T melting curves of 200 nM F-32R-T in 50 mM Tris pH 7.4, 50 mM KCl (curve 1), in the presence of 200 nM (curve 2) or 600 nM (curve 3) porphyrin TMPyP2. Curves 4, 5 and 6 show the melting curves obtained by F-32R-T treated with A1 ($r = 5$); 200 nM TMPyP2 + A1 ($r = 5$); 600 nM TMPyP2 + A1 ($r = 5$), respectively. Exc 475 nm, Em 525 nm; (c) Structures of TMPyP2 and TMPyP4.

translocation steps. Our study suggests that protein A1, being a component of a multiprotein complex formed within NHE (13), may have a similar function for the *KRAS* promoter: i.e. to resolve the folded quadruplex conformations. The destabilizing activity of A1 should facilitate a quadruplex-to-duplex transformation, that seems to be necessary to activate transcription (12,13). To test this hypothesis, we investigated whether the kinetic of hybridization between quadruplex F-32R-T and the complementary 32Y strand becomes faster in the presence of Up1. When quadruplex F-32R-T in 100 mM KCl ($T_m = 70°C$) is mixed at 25°C with the 32Y strand the quadruplex sequence is transformed into the more stable duplex ($T_m = 78°C$) and the fluorescence of the donor increase as in the duplex it is separated from the acceptor (Figure 8a, from A to C). This assembly process can be monitored by measuring the increase of donor (FAM) fluorescence, ΔF, as a function of time ($\Delta F = F - F_0$, where F_0 is the FAM fluorescence at 525 nm at $t = 0$ and F the fluorescence at time t). The ΔF versus t curve shows an exponential shape that was best-fitted to a double-exponential equation (37). For the slow phase a constant k_{slow} of $1.56 \times 10^{-3} \pm 6 \times 10^{-5}\ s^{-1}$ was obtained (Figure 8b). The hybridization performed in the presence of Up1 occurs with a faster kinetic which was nicely best-fitted to a single-exponential equation: $k = 5.2 \times 10^{-3}\ s^{-1}$. In this case the assembly occurs between F-32R-T bound to Up1 and 32Y, the fluorescence increases from B to C (Figure 8b). The half-life $t_{1/2}$ for the hybridization of 32R to 32Y in the presence of Up1 is 133 s, while in the absence of Up1 is 444 s, i.e. more than 3 times higher. This demonstrates that Up1 is indeed a G4-DNA destabilizing protein that facilitates the quadruplex-to-duplex transformation within NHE.

Finally, by a primer extension assay using a template containing the *KRAS* G-rich element we tested whether A1/Up1 is able to remove the block to Taq polymerase caused by quadruplex formation (12,13,24). Figure 9 shows that when the template is incubated in 100 mM KCl prior to primer extension, Taq polymerase is arrested

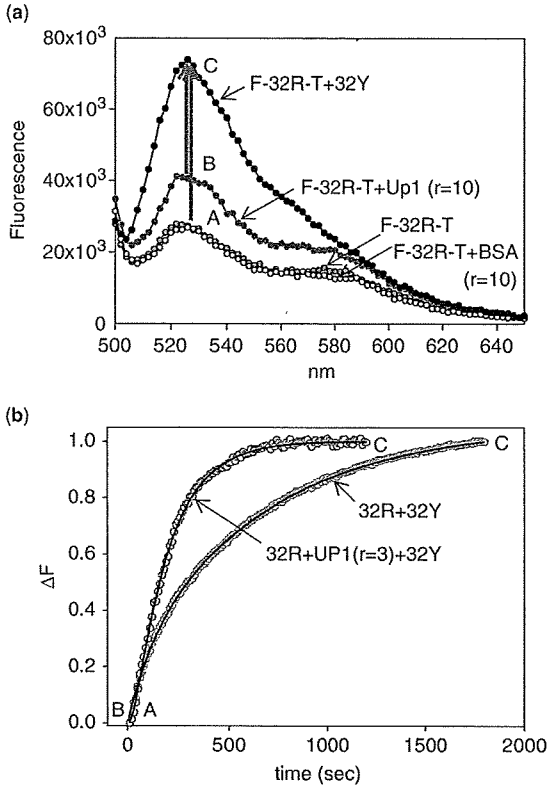

Figure 8. (a) FRET spectra of 200 nM F-32R-T in 50 mM KCl, in the presence of BSA ($r = 10$), Up1 ($r = 10$) and 6-fold complementary 32Y strand. (b) Increase of fluorescence ΔF as a function of time following the addition to 200 nM F-32R-T of 6-fold complementary 32Y in 50 mM Tris pH 7.4, 100 mM KCl. Exc 475 nm; Em 525 nm. The experiment has been conducted in the absence and presence of Up1 ($r = 3$). The solid lines are the best-fits of the experimental points with an exponential equation (SigmaPlot 11, Systat Software Inc).

at the 3′ end of the G-rich tract, as this element folds into a G-quadruplex structure. Contrarily to what we expected, the addition of increasing amounts of protein A1/Up1 strengthened the pause of Taq polymerase. The precise points at which Taq polymerase was arrested were determined by Sanger sequencing reactions and are indicated with arrows in the template sequence. This suggests that A1/Up1 forms with the DNA template a complex which is sufficiently stable to arrest the processivity of Taq polymerase. That's why A1/Up1 enhances the block of Taq polymerase at the G-rich element. However, to corroborate this hypothesis DNA footprinting experiments should be done to demonstrate direct binding of A1/Up1 to the site of arrest. The complex between A1/Up1 and 32R is destabilized when the G-rich strand hybridizes to its complementary sequence to afford a B-DNA duplex for which A1/Up1 has no affinity (see EMSA). Finally, in keeping with the results in Figure 3, the primer-extension assay shows that A1/Up1 binds to the G-rich tract of NHE with a high selectivity, since significant arrests of polymerase at other points of the template are not observed.

DISCUSSION

This work describes the ability of A1, and its derivative Up1, to destabilize the quadruplexes of the *KRAS* promoter and to facilitate their hybridization to the complementary polypyrimidine strand. In accord with pull-down experiments (13), EMSA confirmed that recombinant Up1 and A1 bind to the *KRAS* quadruplex with a high affinity and sequence-specificity, as the binding to other G-quadruplex structures such as *HRAS1*, *HRAS2*, *CMYC*, *VEGF* appeared either weak or inconsistent. Only the quadruplex from the *CKIT* sequence (Table 1) is recognised by Up1. The association of A1 to the *KRAS* promoter is restricted to the polypurine strand, as EMSA shows that A1 does not bind to the complementary polypyrimidine strand, nor to NHE in duplex conformation. Considering that the minimum length for strong binding to Up1 is a stretch of 12 nucleotides (18), 32R, being composed by 32 nucleotides, has potentially two binding sites. In fact, EMSA shows that 32R forms two DNA–protein complexes that are expected to have a stoichiometry of 1:1 and 1:2 (DNA:Up1). This is in accord with the results of Zhang *et al.* (23) showing that Up1 forms with the telomeric repeats $(TTAGGG)_4$ two DNA–protein complexes.

In accord with previous observations (24,25), A1 and Up1 promote a significant reduction of the 260 nm ellipticity, typical of G4-DNA in the parallel conformation. This demonstrates that both proteins are able to unfold the quadruplex structures of the *KRAS* promoter. This conclusion is further supported by FRET-melting experiments showing that the quadruplex formed by F-32R-T is completely disrupted by A1 or Up1. When the *KRAS* G-quadruplex is incubated for 30 min with A1/Up1 before melting, the cooperative transition of the G-quadruplex is replaced by a non-cooperative transition. This suggests that when the *KRAS* sequence is bound to A1/Up1, it is open and in a single-stranded conformation, as shown by the crystal of Up1 with the telomeric repeat (18). In contrast, when a 10-fold excess BSA is added to the G-quadruplex, no change in the quadruplex transition is observed. We interestingly found that protein A1/Up1 facilitates the assembly into a duplex of the two complementary NHE strands. In fact, the half-life of renaturation is reduced from 444 to 133 s in the presence of Up1, 100 mM KCl. This is in accord with earlier studies reporting that A1 promotes a rapid renaturation of nucleic-acid strands, probably by melting the secondary structures that are formed transiently during the annealing process (38). The finding that A1 resolves the *KRAS* quadruplexes has an important biological significance because previous studies supported the notion that the *KRAS* G4-DNA might behave as a transcription suppressor (12,13,28)

The role of A1 *in vivo* has been investigated in the context of the telomere biogenesis (21–23). One possible function of the protein would be to disrupt the G4-DNA structures of the telomere G-repeats, allowing proper elongation by the telomerase (23). The data of our study suggest that A1 could have a similar function in the transcription of *KRAS*. This is in keeping with the fact that A1: (i) binds to the folded G4-DNA conformations of

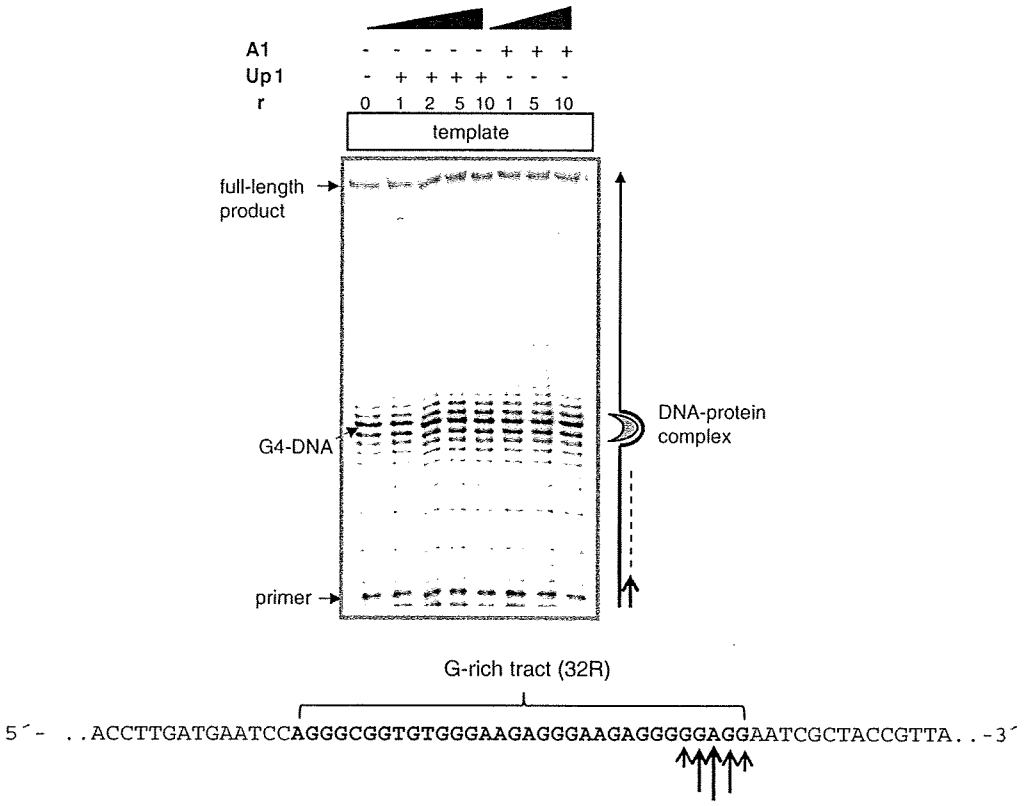

Figure 9. Primer extension assay showing that Taq polymerase pauses at the G-rich element of *KRAS* where the template forms G-quadruplex structures in the presence of KCl. The 87-mer DNA template (100 nM) was mixed with ^{33}P-labelled primer (50 nM) (Table 1) and incubated for 24 h in 140 mM KCl to allow quadruplex formation by the G-rich element. The mixtures were added with increasing amounts of Up1 (lanes 2–5) or A1 (lanes 6–8). *r* = [protein]/[DNA] as specified, and incubated for 30 min prior to primer extension. Taq polymerase is arrested at the G-rich element due to quadruplex formation. In the presence of Up1 or A1 the polymerase arrest is stronger. The points in which Taq polymerase is arrested, have been identified by standard Sanger sequencing reactions. Primer extension reaction performed at 37°C for 1 h. Reaction products separated in a 12% Urea-TBE denaturing gel.

NHE but not to the complementary pyrimidinic strand or duplex NHE; (ii) disrupts G4-DNA and (iii) facilitates the assembly of the NHE strands into a duplex. A possible model for transcription regulation of *KRAS* is the following. NHE should exist in equilibrium between a folded (quadruplex) and a double-stranded conformation. In the folded form the promoter is locked into a form that might inhibit transcription (12,13). To activate transcription, the folded form of NHE should hybridize to the complementary strand in order to restore the duplex. As the quadruplex-to-duplex transformation is likely to be kinetically slow, the functions of A1 would be of destabilizing the quadruplex and allow the G-rich strand to hybridize to its complementary within a time compatible with a response of the cell to molecular stimuli. There are a number of genes with C+G-rich elements in the region surrounding the transcription start site that seems to be characterized by a transcription regulation mechanism involving G-quadruplex structures (12,13,39–45).

Several proteins from different organisms that interact with quadruplex DNA have been reported (46). They can be classified by function into five major groups: (i) proteins that increase the stability of DNA quadruplexes; (ii) proteins that destabilize quadruplex DNA in a non catalytic way; (iii) proteins that unwind catalytically quadruplex DNA in an ATP-dependent fashion; (iv) proteins that promote the formation of quadruplex DNA; (v) Nucleases that specifically cleave DNA at or adjacently to a quadruplex domain. Like other members of the hnRNP family such as hnRNP A2 (20) and CBF-A (20,47) that destabilise the G-quadruplex formed by the d(CGG)n fragile X expanded sequence, protein A1 acts on DNA in a non-catalytic way, i.e. remaining bound to the DNA substrate. Another protein with a similar property is POT-1 which binds to the telomere G-rich DNA overhangs and disrupts G4-DNA structures (48,49). However, contrarily to A1/Up1, POT-1 causes a significant increase of the *P*-value of the quadruplex from the human telomeric repeat, because in the DNA-protein complex the telomeric repeat assumes an extended conformation in which the donor–acceptor are separated by a distance that is too long for FRET (26). Similarly, A1 disrupts the G4-DNA structures assumed by NHE and its remaining bound to the G-rich sequence prevents the DNA from assuming again the folded conformation. We were indeed surprised to observe by primer extension experiments that

at 37°C, A1/Up1 did not remove the block to Taq polymerase and the protein even enhanced the polymerase arrest. This clearly indicates that after interaction the protein remains bound to the template, and the resulting DNA–protein complex is sufficiently strong to arrest the processivity of the polymerase.

Finally, the proposed transcription regulation model suggests two strategies to downregulate the *KRAS* oncogene and sensitize pancreatic cancer cells, which are refractory to conventional treatment, to chemotherapy. First, use of G4-ligands that lock the promoter in the non-transcriptable form by stabilizing the G-quadruplexes; second, use of decoy molecules specific for the proteins that recognize the G4-DNA structure of NHE (28). Work is in progress in our laboratory along this direction.

SUPPLEMENTARY DATA

Supplementary Data are available at NAR Online.

FUNDING

The Italian Association for Cancer Research (AIRC-2008, Associazione Italiana per la Ricerca Contro il Cancro), FVG–Region (Grant-2007); Italian Ministry of University and Research (Prin 2008). Funding for open access charge: AIRC 2008.

Conflict of interest statement. None declared.

REFERENCES

1. Malumbres,M. and Barbacid,M. (2003) RAS oncogenes: the first 30 years. *Nat. Rev. Cancer*, **3**, 459–465.
2. Lowry,D.R. and Willumsen,B.M. (1993) Functional and regulation of ras. *Ann. Rev. Biochem.*, **62**, 851–891.
3. Reuther,G.W. and Der,C.J. (2000) The ras branch of small GTPases: Ras family members don't fall far from the tree. *Curr. Opin. Cell Biol.*, **12**, 157–165.
4. Bos,J.L. (1989) Ras oncogenes in human cancer: a review. *Cancer Res.*, **49**, 4682–4689.
5. Barbacid,M. (1990) Ras oncogenes: their role in neoplasia. *Eur. J. Clin. Invest.*, **20**, 225–235.
6. Burmer,G.C. and Loeb.L.A. (1989) Mutations in the KRAS2 oncogene during progressive stages of human colon carcinoma. *Proc. Natl Acad. Sci. USA*, **86**, 2403–2407.
7. Almoguerra,C., Shibata.D., Forrester,K., Martin,J., Arnheim,N. and Perucho.M. (1988) Most human carcinomas of the exocrine pancreas contain mutant c-K-ras genes. *Cell*, **53**, 549–554.
8. Shirasawa,S., Furuse,M., Yokoyama,N. and Sasazuki,T. (1993) Altered growth of human colon cancer cell lines disrupted at activated Ki-ras. *Science*, **260**, 85–88.
9. Schubbert,S., Shannon,K. and Bollag.G. (2007) Hyperactive Ras in developmental disorders and cancer. *Nat. Rev.*, **7**, 295–308.
10. Bardeesy,N. and DePinho.R. (2002) Pancreatic cancer biology and genetics. *Nat. Rev.*, **2**, 897–909.
11. Yamamoto,F. and Perucho.M. (1988) Characterization of the human c-K-ras gene promoter. *Oncogene Res.*, **3**, 125–138.
12. Cogoi,S. and Xodo,L. (2006) G-quadruplex formation within the promoter of the KRAS proto-oncogene and its effect on transcription. *Nucleic Acids Res.*, **34**, 2536–2549.
13. Cogoi,S., Paramasivam.M., Spolaore,B. and Xodo.L.E. (2008) Structural polymorphism within a regulatory element of the human KRAS promoter: formation of G4-DNA recognized by nuclear proteins. *Nucleic Acids Res.*, **36**, 3765–3780.
14. Dreyfuss,G., Matunis,S., Pinol-Roma,S. and Burd,C. (1993) hnRNP proteins and the biogenesis of mRNA. *Annu. Rev. Biochim.*, **62**, 289–321.
15. McAfee,J., Huang,M., Soltaninassad,S., Rech,J., Iyengar,S. and Lestougeon,W. (1997) The packaging of pre-mRNA. In Krainer,A.R. (ed.), *Eukaryotic mRNA Processing*. Vol. 17, IRL Press at Oxford University Press, New York, N.Y., pp. 68–102.
16. Cobianchi,F., SenGupta,D., Zmudzka,B. and Wilson,S. (1986) Structure of rodent helix-destabilizing protein revealed by cDNA cloning. *J. Biol. Chem.*, **261**, 3536–3543.
17. Shamoo,Y., Abdul-Manan,N., Patten,A., Crawford,J., Pellegrini,M. and Williams,K.R. (1994) Both RNA-binding domains in heterogenous nuclear ribonucleoprotein A1 contribute toward single-stranded-RNA binding. *Biochemistry*, **33**, 8272–8281.
18. Ding,J., Hayashi,M., Zhang,Y., Manche,L., Krainer,A. and Xu,R.-M. (1999) Crystal structure of the two-RRM domain of vhnRHP A1 (Up1) complexed with single-stranded telomeric DNA. *Genes Dev.*, **13**, 1102–1115.
19. Fiset,S. and Chabot,B. (2001) hnRNP A1 may interact simultaneously with telomeric DNA and the human telomerase RNA in vitro. *Nucleic Acids Res.*, **29**, 2268–2275.
20. Khateb,S., Weisman-Shomer,P., Hershco,I., Loeb,L.A. and Fry,M. (2004) Destabilization of tetraplex structures of the fragile X repeat sequence (CGG)n is mediated by homolog-conserved domains in three members of the hnRNP family. *Nucleic Acids Res.*, **32**, 4145–4154.
21. LaBrance,H., Dupuis,S., Ben-David,Y., Bani,M.-R., Wellinger,R. and Chabot,B. (1998) Telomere elongation by hnRNP A1 and a derivative that interacts with telomeric repeats and telomerase. *Nat. Genet.*, **19**, 199–202.
22. Riva,S., Morandi,C., Tsoulfas,P., Pandolfo,M., Biamonti,G., Merill,B., Williams,K., Multhaup,G., Beyreuther,K., Werr,H. *et al.* (1986) Mammalian single-stranded DNA binding protein UP I is derived from the hnRNP core protein A1. *EMBO J.*, **5**, 2267–2273.
23. Zhang,Q., Manche,L., Xu,R.-M. and Krainer,A. (2006) hnRNP A1 associates with telomere ends and stimulates telomerase activity. *RNA*, **12**, 1116–1128.
24. Fukuda,H., Katahira,M., Tsuchiya,N., Enokizono,Y., Sugimura,M., Nagao,M. and Nakagama,H. (2002) Unfolding of quadruplex structure in the G-rich strand of the minisatellite repeat by the binding protein UP1. *Proc. Natl Acad. Sci. USA*, **99**, 12685–12690.
25. Fukuda,H., Katahira,M., Tanaka,E., Enokizono,Y., Tsuchiya,N., Higuchi,K., Nagao,M. and Nakagama,H. (2005) Unfolding of higher DNA structures formed by the d(CGG) triplet repeat by UP1 protein. *Genes Cells*, **10**, 953–962.
26. Salas,T.R., Petruseva,I., Lavrik,O., Bourdoncle,A., Mergny,J.L., Favre,A. and Saintomé.C. (2006) Human replication protein A unfolds telomeric G-quadruplexes. *Nucleic Acids Res.*, **34**, 4857–4865.
27. Nagatoishi,S., Nojima,T., Galezowska,E., Juskowiak,B. and Takenaka,S. (2006) G quadruplex-based FRET probes with the thrombin-binding aptamer (TBA) sequence designed for the efficient fluorometric detection of the potassium ion. *Chembiochem*, **7**, 1730–1737.
28. Cogoi,S., Paramasivam,M., Filichev,V., Géci,I., Pedersen.E.B. and Xodo,L.E. (2009) Identification of a new G-quadruplex motif in the *KRAS* promoter and design of TINA-modified G4-decoys with antiproliferative activity in pancreatic cancer cells. *J. Med. Chem.*, **52**, 564–568.
29. Seenisamy,J., Rezler,E.M., Powell,T.J., Tye,D., Gokhale,V., Joshi,C.S., Siddiqui-Jain,A. and Hurley,L.H. (2004) The dynamic character of the G-quadruplex element in the c-MYC promoter and modification by TMPyP4. *J. Am. Chem. Soc.*, **126**, 8702–8709.
30. Phan,A.T., Modi,Y.S. and Patel,D.J. (2004) Propeller-type parallel-stranded G-quadruplexes in the human c-myc promoter. *J. Am. Chem. Soc.*, **126**, 8710–8716.
31. Phan,A.T., Kuryavyi,V., Burge,S., Neidle,S. and Patel,D.J. (2007) Structure of an unprecedented G-quadruplex scaffold in the human c-kit promoter. *J. Am. Chem. Soc.*, **129**, 4386–4392.
32. Guo,K., Gokhale,V., Hurley,L.H. and Sun,D. (2008) Intramolecularly folded G-quadruplex and i-motif structures in the proximal promoter of the vascular endothelial growth factor gene. *Nucleic Acids Res.*, **36**, 4598–4608.

33. Rujan,I.N., Meleney,J.C. and Bolton,P.H. (2005) Vertebrate telomere repeat DNAs favor external loop propeller quadruplex structures in the presence of high concentrations of potassium. *Nucleic Acids Res.*, **33**, 2022–2031.
34. Clegg,R.M. (1992) Fluorescence resonance energy transfer and nucleic acids. *Methods Enzymol.*, **211**, 353–388.
35. Kankia,B.I., Barany,G. and Musier-Forsyth,K. (2005) Unfolding of DNA quadruplexes induced by HIV-1 nucleocapsid protein. *Nucleic Acids Res.*, **33**, 4395–4403.
36. Han,H., Langley,D.R., Rangan,A. and Hurley,L.H. (2001) Selective interactions of cationic porphyrins with G-quadruplex structures. *J. Am. Chem. Soc.*, **123**, 8902–8913.
37. Green,J.J., Ying,L., Klenerman,D. and Balasubramanian,S. (2003) Kinetics of unfolding the humna telomeric DNA G-quartet structure using a PNA trap. *J. Am. Chem. Soc.*, **125**, 3763–3767.
38. Pontius,B.W. and Berg,P. (1990) Renaturation of complementray DNA strands mediated by puyrified mammalian heterogeneous nuclear ribonucleoprotein A1 protein: implications for a mechanism for rapid molecular assembly. *Proc. Natl. Acad. Sci USA*, **87**, 8403–8407.
39. Siddiqui-Jain,A., Grand,C.L., Bearss,D.J. and Hurley,L.H. (2002) Direct evidence for a G-quadruplex in a promoter region and its targeting with a small molecule to repress c-CMYC transcription. *Proc. Natl Acad. Sci. USA*, **99**, 11593–11598.
40. Eddy,J. and Maizels,N. (2006) Gene function correlates with potential for G4 DNA formation in the human genome. *Nucleic Acids Res.*, **34**, 3887–3896.
41. Huppert,J.L. and Balasubramanian,S. (2007) G-quadruplexes in promoters throughout the human genome. *Nucleic Acids Res.*, **35**, 406–413.
42. Palumbo,S.L., Memmott,R.M., Uribe,D.J., Krotova-Khan,Y., Hurley,L.H. and Ebbinghaus,S.W. (2008) A novel G-quadruplex-forming GGA repeat region in the c-myb promoter is a critical regulator of promoter activity. *Nucleic Acids Res.*, **36**, 1755–1769.
43. Shklover,J., Etzioni,S., Weisman-Shomer,P., Yafe,A., Bengal,E. and Fry,M. (2008) MyoD uses overlapping but distinct elements to bind E-box and tetraplex structures of regulatory sequences of muscle-specific genes. *Nucleic Acids Res.*, **35**, 7087–7095.
44. Todd,A.K. and Neidle,S. (2008) The relationship of potential G-quadruplex sequences in cis-upstream regions of the human genome to SP1-binding elements. *Nucleic Acids Res.*, **36**, 2700–2704.
45. Sun,D., Liu,W.J., Guo,K., Rusche,J.J., Ebbinghaus,S., Gokhale,V. and Hurley,L.H. (2008) The proximal promoter region of the human vascular endothelial growth factor gene has a G-quadruplex structure that can be targeted by G-quadruplex-interactive agents. *Mol. Cancer Ther.*, **7**, 880–889.
46. Fry,M. (2007) Tetraplex DNA and its interacting proteins. *Front. Biosci.*, **12**, 4336–4351.
47. Weisman-Shomer,P., Cohen,E. and Fry,M. (2002) Distinct domains in the CarG-box binding factor-A destabilize tetraplex forms of the fragile X expanded sequence d(CGG)n. *Nucleic Acids Res.*, **30**, 3672–3681.
48. Zaug,A.J., Podell,E.R. and Cech,T.R. (2005) Human POT1 disrupts telomeric G-quadruplexes allowing telomerase extension in vitro. *Proc. Natl. Acad. Sci. USA*, **102**, 10864–10869.
49. Wang,F., Podell,E.R., Zaug,A.J., Yang,Y., Baciu,P., Cech,T.R. and Lei,M. (2007) The POT1-TPP1 telomere complex is a telomerase processivity factor. *Nature*, **445**, 506–510.

FEBS Letters 583 (2009) 2710–2714

ELSEVIER

FEBS Letters

journal homepage: www.FEBSLetters.org

Mdmx enhances p53 ubiquitination by altering the substrate preference of the Mdm2 ubiquitin ligase

Koji Okamoto [a,b,c], Yoichi Taya [b,c,1], Hitoshi Nakagama [a,*]

[a] National Cancer Center Research Institute, Early Oncogenesis Research Project, 5-1-1 Tsukiji, Chuo-ku, Tokyo 104-0045, Japan
[b] National Cancer Center Research Institute, Radiobiology Division, 5-1-1 Tsukiji, Chuo-ku, Tokyo 104-0045, Japan
[c] SORST, Japan Science and Technology Corporation, Japan

ARTICLE INFO

Article history:
Received 11 May 2009
Revised 26 June 2009
Accepted 13 July 2009
Available online 18 July 2009

Edited by Noboru Mizushima

Keywords:
Mdmx
Mdm2
p53
Ubiquitination

ABSTRACT

mdm2 and _mdmx_ oncogenes play essential yet non-redundant roles in synergistic inactivation of the tumor suppressor, p53. While Mdm2 inhibits p53 activity mainly by augmenting its ubiquitination, the functional role of Mdmx on p53 ubiquitination remains obscure. In transfected H1299 cells, Mdmx augmented Mdm2-mediated ubiquitination of p53. In in vitro ubiquitination assays, the Mdmx/Mdm2 heteromeric complex, in comparison to the Mdm2 homomer, showed enhanced ubiquitinase activity toward p53 and the reduced auto-ubiquitination of Mdm2. Alteration of the substrate specificity via binding to Mdmx may contribute to efficient ubiquitination and inactivation of p53 by Mdm2.

Structured summary:
MINT-7219995: *P53* (uniprotkb:P04637) *physically interacts* (MI:0914) with *Ubiquitin* (uniprotkb:P62988) by *anti bait coimmunoprecipitation* (MI:0006)
MINT-7220023: *Ubiquitin* (uniprotkb:P62988) *physically interacts* (MI:0914) with *P53* (uniprotkb:P04637) by *pull down* (MI:0096)

1. Introduction

The p53 tumor suppressor protein plays a central role in preventing tumorigenesis. p53 functions as a sequence-specific transcriptional factor [1,2], and activated p53 exerts its function as a tumor suppressor by inducing numerous target genes [3–6]. In most cancer cells, its activity is lost via alteration of its gene or via other cellular events that inactivate p53 [7–9].

Mdm2 and Mdmx function as two major players in the suppression of p53 activity [10]. Accumulating reports indicate that the major function of Mdm2 in suppressing p53 is attributed to Mdm2-dependent p53 ubiquitination, which triggers proteasomal degradation or nuclear export of p53 [11], although it has been reported that Mdm2 inactivates p53 by other mechanisms [12–15]. Mdm2 possesses a RING finger domain, a protein–protein interaction motif that is found in many eukaryotic proteins and often possesses E3 ubiquitin ligase activity [16]. Indeed, Mdm2 functions as an E3 ubiquitin ligase, and the RING domain of Mdm2 is essential for its ubiquitin ligase activity toward p53 and Mdm2 itself [17–19].

Mdmx shares an extensive structural homology with Mdm2, and forms a heterodimer complex with Mdm2 through their RING finger domains [20,21], yet Mdmx in itself lacks the robust activity of an E3 ubiquitin ligase [22]. Thus, both genetic and biochemical evidence indicates that Mdmx and Mdm2 perform distinct yet co-operative functions in p53 inactivation.

Recent reports suggest that Mdmx may inactivate p53 by augmenting Mdm2-mediated ubiquitination of p53 [23–25]. However, precise mechanism by which Mdmx stimulates p53 ubiquitination by Mdm2 is not yet known.

In this paper, we demonstrated that wild-type Mdmx is capable of enhancing Mdm2-mediated p53 ubiquitination in vivo. Further, the in vitro study using purified Mdm2 or the Mdm2/Mdmx complex revealed that, when complexed with Mdmx, the extent of p53 ubiquitination by Mdm2 was enhanced while poly-ubiquitination of Mdm2 was significantly decreased. We propose that the effect of Mdmx on the preference of the substrate of the Mdm2 ubiquitin ligase plays an important role in effective ubiquitination of p53.

* Corresponding author.
E-mail address: hnakagam@ncc.go.jp (H. Nakagama).
[1] Present address: Cancer Science Institute of Singapore, National University of Singapore, Singapore 117456, Singapore.

0014-5793/$36.00 © 2009 Federation of European Biochemical Societies. Published by Elsevier B.V. All rights reserved.
doi:10.1016/j.febslet.2009.07.021

2. Materials and methods

2.1. DNA transfection

In DNA transfection experiments using H1299 cells, 2 μg of DNA and 4 μl of Lipofectamine 2000 reagent (Invitrogen) were introduced per 2.0×10^5 cells according to manufacturer's protocol. Cells were then incubated for 20 h before harvesting.

2.2. In vivo ubiquitination assay

For detection of p53 conjugated with endogenous ubiquitin, in vivo ubiquitination assays were performed as previously described [26] with some modifications. Transfected H1299 cells were lysed in SDS lysis buffer (50 mM Tris, pH 7.5, 100 mM NaCl, 1% SDS) supplemented with 1 mM DTT and protease inhibitor cocktail (PI) [27], boiled for 10 min, and diluted with ×4 volumes of dilution buffer (50 mM Tris, pH 7.5, 100 mM NaCl, 1.25% Triton X-100) supplemented with DTT and PI. After sonication of the lysates, p53 was immunoprecipitated with anti-p53 antibody (DO-1). Subsequently the immunoprecipitates were washed three times with 200-NP buffer [27], and analyzed by Western blotting with DO-1 and anti-ubiquitin antibody (FK2, MBL).

For detection of p53 conjugated with transfected $(His)_6$-ubiquitin, transfected H1299 cells were lysed in urea lysis buffer (100 mM NaH2PO4, 10 mM Tris–HCl, pH 8.0, 500 mM NaCl, 10% glycerol, 0.1% Triton X-100, 10 mM imidazole) supplemented with 10 mM β-mercaptoethanol, PI, 5 mM Iodoacetamide, and 1 mg/ml NEM. Proteins conjugated with His-tagged ubiquitin were purified as described before [28], and analyzed by Western blot analysis.

2.3. Protein expression and purification

Flag-tagged Human Mdm2 (Flag-Mdm2) or Human Mdmx RNA was transcribed from the corresponding cDNA using the Wheat Germ Expression Kit (Cell Free Science, Japan). Subsequently, the Flag-Mdm2 RNA alone or in combination with an excess amount of the Mdmx RNA was used for in vitro translation with wheat germ lysate (Cell Free Science) according to the manufacturer's instructions. Flag-Mdm2 or the Flag-Mdm2/Mdmx complex was then purified on agarose conjugated with anti-Flag antibody.

2.4. In vitro ubiquitination assay

In vitro ubiquitination assays were performed as previously described with some modifications [29]. Approximately 100 ng of Flag-Mdm2 or the Flag-Mdm2/Mdmx complex were mixed with the following purified components; 8 ng of GST-p53, 10 ng of E1 (Boston Biochem), 80 ng of E2 (UbcH5b, Boston Biochem), 3 μg of His-ubiquitin (Calbiochem), or methylated ubiquitin (Boston Biochem). In experiments shown in Fig. 4D, ^{125}I-ubiquitin (Perkin–Elmer) was included in the reaction mixture. These components were incubated in a reaction buffer (40 mM Tris–HCl, pH 7.5, 5 mM $MgCl_2$, 10 mM NaCl) in the presence of 2 mM Mg–ATP at 37 °C for the indicated times. After the reactions were terminated by adding SDS sample buffer, ubiquitinated proteins were separated in SDS–PAGE gels and detected by Western blot analyses or autoradiography.

3. Results

3.1. Wild-type Mdmx was capable of enhancing p53 ubiquitination in the presence of Mdm2 in vivo

Recently, we demonstrated that the non-phosphorylatable, active form of Mdmx augments p53 ubiquitination mediated by wild-type Mdm2 in transfected H1299 cells [30]. In order to determine whether wild-type Mdmx cooperates with Mdm2 to induce ubiquitination of p53 as well, wild-type Mdmx (Mdmx-wt) or the non-phosphorylated form of Mdmx (Mdmx-3A) was transfected together with Mdm2 into H1299 cells, and conjugation of p53 with endogenous ubiquitin was examined by Western blot analyses (Fig. 1). As expected from previous observation [30], Mdmx-3A, which is resistant to Mdm2-mediated ubiquitination and degradation, was expressed at higher levels than wild-type Mdmx (Fig. 1, lanes 2 and 3). p53 ubiquitination induced by Mdm2 was enhanced in the presence of co-transfected wild-type Mdmx (Fig. 1, lanes 5 and 8), indicating that wild-type Mdmx is capable of stimulating Mdm2-mediated ubiquitination of p53,

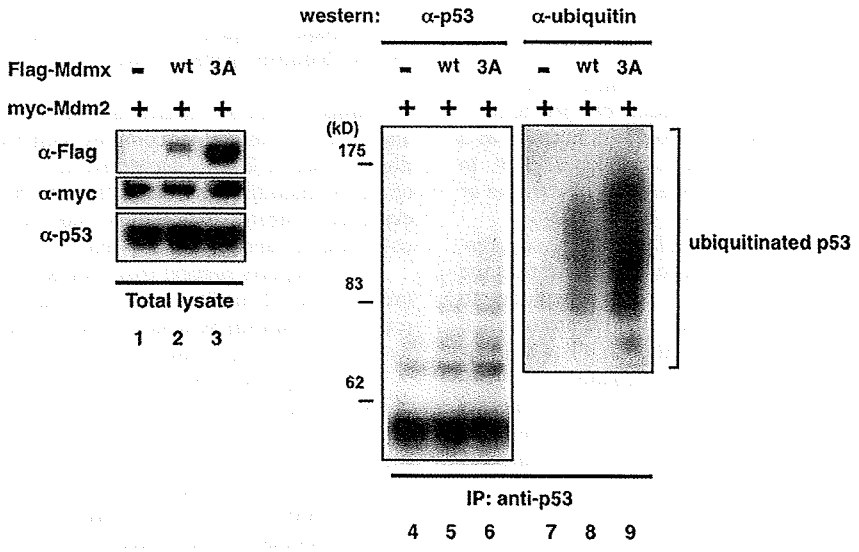

Fig. 1. Mdmx cooperates with Mdm2 to induce p53 ubiquitination. HA-p53 (0.15 mg) and either 0.4 mg of the control vector, wild-type Flag-Mdmx, or the Flag-Mdmx-3A mutant were transfected into H1299 cells in the presence of 0.2 mg of Myc-Mdm2. The total amount of transfected DNA was adjusted to 2 μg with pBluescript plasmid (Stratagene). Twenty hours after transfection, lysates prepared under denaturing conditions were used for immunoprecipitaiton with anti-p53 (DO-1) antibody. The immunoprecipitates were then used for Western blot analyses with DO-1 (left panel, and right bottom panel for low exposure) and with anti-ubiquitin antibody (right panel). Amounts of immunoprecipitates used for Western were normalized such that an equal amount of non-ubiquitinated p53 was loaded in each lane.

although the extent of the stimulation is less than that induced by the non-phosphorylatable mutant (Fig. 1, lanes 6 and 9).

3.2. Mutation at the C-terminal ubiquitinated lysines largely abolished p53 ubiquitination by Mdmx

It has been documented that Mdm2 ubiquitinates p53 at the six C-terminal lysines, the integrity of which are required for its nuclear export [31,32]. We created a mutant p53 in which all six lysines at the C-terminal domain (Fig. S1) were substituted by arginine (p53-K6R), and introduced wild-type p53 or the K6R mutant into H1299 cells together with Mdm2 in the presence or absence of Mdmx-3A. Examination of p53 ubiquitination in vivo revealed that the K6R mutation eliminates a majority of p53 ubiquitination enhanced by Mdmx (Fig. S2), indicating the six lysines were major sites for Mdmx-dependent ubiquitination.

3.3. Association of Mdmx with Mdm2 augments the ability of Mdm2 to ubiquitinate p53 and inhibits poly-ubiquitination of Mdm2 in vitro

In order to determine whether Mdmx enhances Mdm2-dependent ubiquitination of p53 via direct association with Mdm2, we next performed in vitro ubiquitination assays using purified recombinant proteins of Mdm2 or an Mdm2/Mdmx complex (see Section 2). Silver staining of the purified proteins indicated that the co-purified Mdmx formed a complex with Mdm2 at approximately a 1:1 molar ratio (Fig. 2A, right panel).

In order to determine the effect of the association with Mdmx on the activity of E3 ubiquitin ligase of Mdm2, homomeric Mdm2 or the Mdmx/Mdm2 complex was incubated with E1, E2 (UbcH5b), GST-p53, and ubiquitin, and time-course analyses of the ubiquitination of p53 and auto-ubiquitination of Mdm2 were simultaneously performed. The complex formation of Mdm2 with Mdmx-3A or with wild-type Mdmx resulted in an increase of p53 ubiquitination (Fig. 2B and C). In contrast, the Mdmx/Mdm2 complex showed a marked decrease in poly-ubiquitinated forms of Mdm2 in comparison to homomeric Mdm2 (Fig. 2B and C), indicating that the association with Mdmx-3A augments Mdm2-dependent p53 ubiquitination while it inhibits poly-ubiquitination of Mdm2.

3.4. Mdmx inhibits ubiquitination of the Mdm2-containing enzymatic complex

In order to confirm that Mdmx inhibits auto-ubiquitination of Mdm2, in vitro ubiquitination assays of the Mdm2 homomer or the Mdm2/Mdmx complex were performed in the presence of

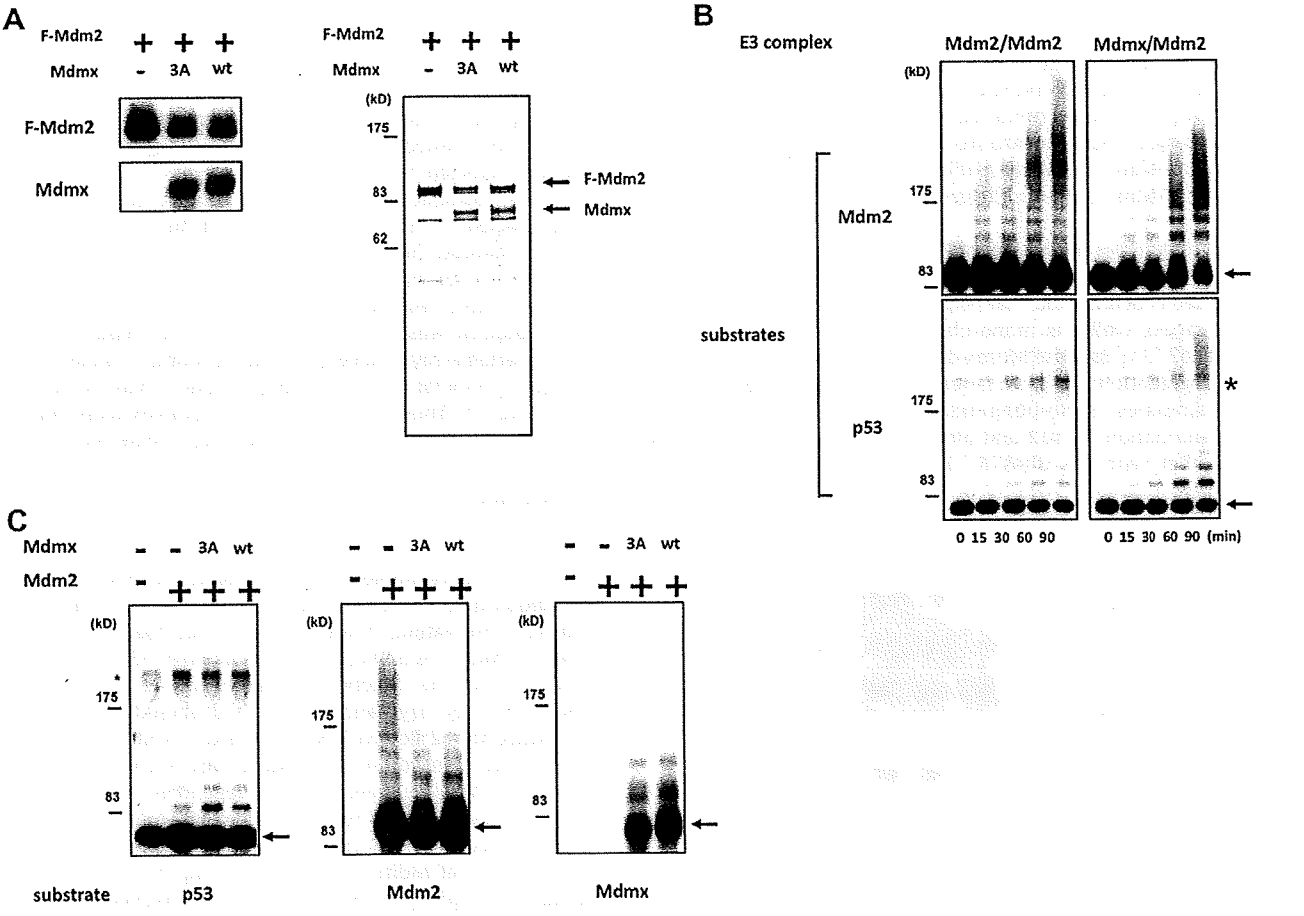

Fig. 2. Association of Mdmx with Mdm2 augments the activity of Mdm2 to ubiquitinate p53 and inhibits auto-ubiquitination of Mdm2 in vitro. (A) Purification of Mdm2 and the Mdm2/Mdmx complex. Flag-tagged Mdm2 was translated alone, or co-translated with Mdmx-3A or wild-type Mdmx in wheat germ lysates, as described in Section 2. The purified proteins were separated by10% SDS–PAGE, and detected by silver staining (right panel), or by Western blotting analyses with anti-Flag antibody (M2) or anti-Mdmx antibody (D-19) (left panel). (B) *In vitro* ubiquitination assays were performed with purified Mdm2 or Mdmx-3A/Mdm2. Ubiquitination reactions were terminated at the indicated times, and the extent of p53 ubiquitination and Mdm2 auto-ubiquitination was evaluated by Western blot analyses with anti-Flag antibody or anti-p53 antibody. The position of non-ubiquitinated substrates is designated by arrows. (C) In vitro ubiquitination assays were performed as described in (B), and the ubiquitination reactions were terminated after 30 min. Ubiquitination of Mdmx, p53, and Mdm2 was evaluated by Western blot analyses.

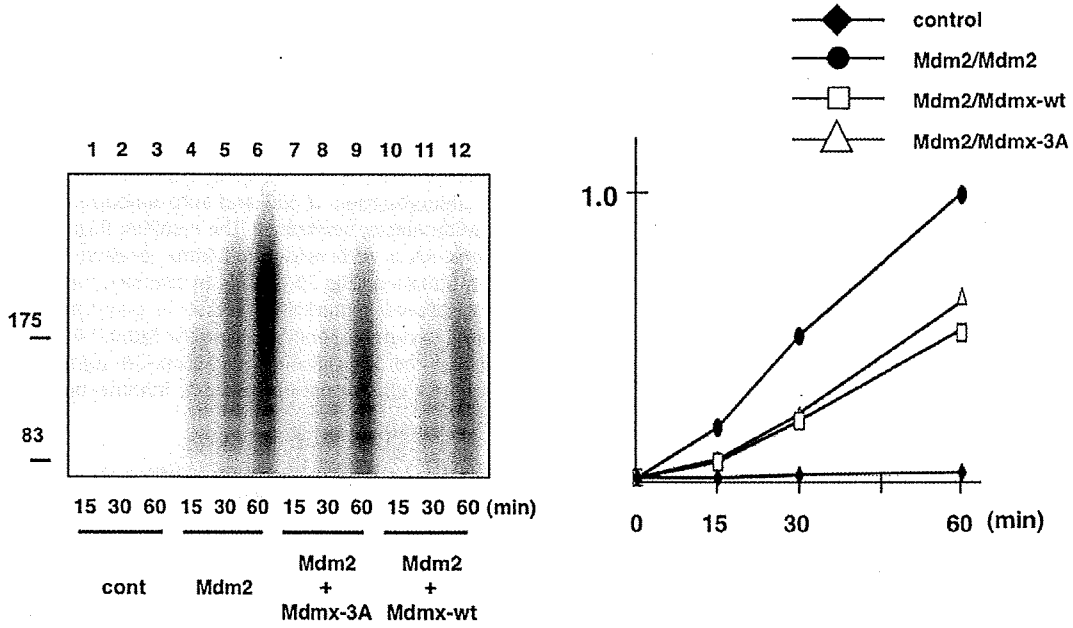

Fig. 3. In vitro ubiquitination reaction was performed as described in Fig. 2C, except that ^{125}I-labeled ubiquitin was included in the reaction. (left panel) Ubiquitinated Mdm2 or Mdm2/Mdmx was separated by 10% SDS–PAGE, and detected by autoradiography. Note that the ladder represents a mixture of ubiqutination of Mdm2 and Mdmx in lanes 7–12 (left panel). Levels of the ubiquitination were quantified and relative levels of ubiquitination were plotted (right panel).

^{125}I-labeled ubiquitin. Quantification of ubiquitin attached to the enzymatic complexes demonstrated that the auto-ubiquitination of the Mdm2 was indeed hindered by the complex formation with either wild-type Mdmx or Mdmx-3A (Fig. 3). Thus, the complex formation of Mdm2 with Mdmx affects the preference for the substrate of the Mdm2 ubiquitin ligase.

3.5. *Mdmx stimulates Mdm2-dependent mono-ubiquitination of p53*

It has been documented that poly-ubiquitination of p53 induces its degradation, while its mono-ubiquitnation stimulates nuclear export of p53 [33]. Because Mdmx does not significantly contribute to p53 degradation [34], we attempted to determine whether Mdmx stimulates mono-ubiquitination of p53 rather than its poly-ubiquitination. Mdm2 and p53 were introduced into H1299 cells together with His-Ub-K7R, $(His)_6$-tagged mutant ubiquitin which is not capable of forming a ladder of poly-ubiquitination due to arginine substitution in all seven lysine residues [29]. Subsequently, His-Ub-K7R was purified from lysates that were prepared from transfected cells, and p53 conjugated with His-Ub-7KR was detected by Western blot analyses with anti-p53 antibody. The introduction of wild-type Mdmx augmented mono-ubiquitination of p53 (Fig. 4, lane 2), and the Mdmx-3A mutation further enhanced the p53 mono-ubiquitination (Fig. 4, lane 3).

In order to determine whether Mdmx stimulates Mdm2-dependent mono-ubiquitination of p53 in vitro as well as in vivo, methylated ubiquitin was used instead of wild-type ubiquitin in in vitro ubiquitination assays. Indeed, the Mdmx/Mdm2 complex showed a stronger activity for p53 mono-ubiquitination than the homomeric Mdm2 (Fig. S3). Thus, the formation of a complex with Mdmx augments the activity of Mdm2 to mono-ubiquitinate p53.

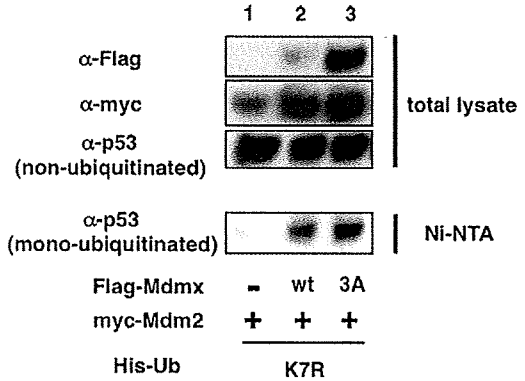

Fig. 4. Mdmx-3A or the control vector was transfected into H1299 cells together with Myc-Mdm2, HA-p53 and the indicated $(His)_6$-tagged ubiquitin K7R mutant. Twenty hours after transfection, cells were lysed with a buffer containing 6 M urea, and normalized lysates that contain equal amounts of non-ubiquitinated p53 were used to purify His-tagged ubiquitin on Ni-NTA agarose (QIAGEN). Ubiquitinated p53 was detected by Western blot analysis with anti-p53 antibody (DO-1).

4. Discussion

In this report, we demonstrated that wild-type Mdmx as well as its non-phosphorylatable mutant cooperates with Mdm2 to stimulate ubiquitination of p53 both in vivo and in vitro. In agreement with our observation, it was reported that Mdmx enhances the activity of Mdm2 as a ubiquitin ligase in vitro [35]. Mdmx complements the catalytic function of mutant Mdm2 proteins that are deficient in the enzymatic activity as a ubiquitin ligase [23–25] and Mdmx/Mdm2 hetero-RING complexes exhibit a greater E3 ligase activity than homomeric Mdm2 [36]. Such effects of Mdmx on Mdm2 should enhance Mdm2-dependent ubiquitination of p53, consistent with the role of Mdmx as an inhibitor of p53.

It was previously reported that Mdmx augments not only auto-ubiquitination of Mdm2 but also the ubiquitin ligase activity of Mdm2 toward p53 [35] in in vitro assays. However, auto-ubiquitination of the Mdm2 ubiquitin ligase negatively affects its activity because poly-ubiquitinated Mdm2 is targeted for proteasome-mediated degradation. Therefore, enhanced ubiquitinase activity of Mdm2 by Mdmx may not be translated into efficient stimulation of p53 ubiquitination if the association of Mdmx to Mdm2 simultaneously leads to stimulation of self-destruction of Mdm2. Our

observation that Mdmx inhibits poly-ubiquitination of Mdm2 while it stimulates p53 ubiquitination may attribute to a mechanism by which Mdmx stimulates Mdm2-dependent p53 ubiquitination without enhanced destruction of Mdm2, thus providing the molecular basis of how Mdmx cooperates with Mdm2 to inhibit p53 activity.

Recently Linke et al. reported the crystal structure of the heterodimer of Mdmx/Mdm2 RING domain, and proposed a model that favors transfer of ubiquitin to Mdmx that does not interact with E2 [37]. This can explain why Mdm2 is not extensively ubiquitinated in the Mdmx/Mdm2 heteromeric complex, thus providing mechanistic basis for reduced ubiquitination of Mdm2 in the Mdmx/Mdm2 complex (Fig. 2). It is noteworthy that, in in vitro ubiquitination assays, the levels of Mdm2 ubiquitination in the homomeric Mdm2 are higher than combined levels of ubiquitination of Mdm2 and Mdmx in the heteromeric complex (Fig. 3). Therefore, it is likely that Mdmx is relatively resistant to ubiquitination by bound Mdm2, unless Mdmx undergoes specific modification such as phosphorylation [27].

It is not clear at this moment how Mdmx stimulates Mdm2-mediated ubiquitination of p53. Mdm2 bound to Mdmx may position its catalytic domain more closer to the C-terminal domain of p53 than homomeric Mdm2, resulting in enhanced p53 ubiquitination. Alternatively, Mdm2 or Mdmx may compete with p53 as a substrate for Mdm2, and relative resistance of Mdmx against ubiquitination by bound Mdm2 may translate into facilitated p53 ubiquitination. Presumably, these two possibilities are not mutually exclusive, and combined effects of Mdmx on Mdm2-mediated ubiquitination may serve to stimulate ubiquitination and inactivation of p53.

Acknowledgements

We thank Aart Jochemsen for helpful suggestions. The His-ubiquitin expression plasmids were kind gifts from Wei Gu. We thank Kenji Kashima and Chihiro Ohtsubo for experimental assistance. This work was supported by a Grant-in-Aid for Scientific Research from the Ministry of Education, Culture, Sports, Science and Technology of Japan (Y.T and K.O.), a Grant-in-Aid for Third Term Comprehensive Control Research for Cancer from the Ministry of Health, Labor and Welfare, Japan (Y.T.), and the Foundation for Promotion of Cancer Research (K.O.).

Appendix A. Supplementary data

Supplementary data associated with this article can be found, in the online version, at doi:10.1016/j.febslet.2009.07.021.

References

[1] Levine, A.J. (1997) P53, the cellular gatekeeper for growth and division. Cell 88, 323–331.
[2] Laptenko, O. and Prives, C. (2006) Transcriptional regulation by p53: one protein, many possibilities. Cell Death Differ. 13, 951–961.
[3] Levine, A.J., Hu, W. and Feng, Z. (2006) The P53 pathway: what questions remain to be explored? Cell Death Differ. 13, 1027–1036.
[4] Oren, M. (2003) Decision making by p53: life, death and cancer. Cell Death Differ. 10, 431–442.
[5] Ko, L.J. and Prives, C. (1996) P53: puzzle and paradigm. Genes Dev. 10, 1054–1072.
[6] Vogelstein, B., Lane, D. and Levine, A.J. (2000) Surfing the p53 network. Nature 408, 307–310.
[7] Lozano, G. and Zambetti, G.P. (2005) What have animal models taught us about the p53 pathway? J. Pathol. 205, 206–220.
[8] Vousden, K.H. and Lu, X. (2002) Live or let die: the cell's response to p53. Nat. Rev. Cancer 2, 594–604.
[9] Olivier, M., Eeles, R., Hollstein, M., Khan, M.A., Harris, C.C. and Hainaut, P. (2002) The IARC TP53 database: new online mutation analysis and recommendations to users. Hum. Mutat. 19, 607–614.
[10] Marine, J.C., Francoz, S., Maetens, M., Wahl, G., Toledo, F. and Lozano, G. (2006) Keeping p53 in check: essential and synergistic functions of Mdm2 and Mdm4. Cell Death Differ. 13, 927–934.
[11] Michael, D. and Oren, M. (2003) The p53-Mdm2 module and the ubiquitin system. Semin. Cancer Biol. 13, 49–58.
[12] Momand, J., Zambetti, G.P., Olson, D.C., George, D. and Levine, A.J. (1992) The mdm-2 oncogene product forms a complex with the p53 protein and inhibits p53-mediated transactivation. Cell 69, 1237–1245.
[13] Oliner, J.D., Pietenpol, J.A., Thiagalingam, S., Gyuris, J., Kinzler, K.W. and Vogelstein, B. (1993) Oncoprotein MDM2 conceals the activation domain of tumour suppressor p53. Nature 362, 857–860.
[14] Ito, A., Lai, C.H., Zhao, X., Saito, S., Hamilton, M.H., Appella, E. and Yao, T.P. (2001) P300/CBP-mediated p53 acetylation is commonly induced by p53-activating agents and inhibited by MDM2. Embo J. 20, 1331–1340.
[15] Kobet, E., Zeng, X., Zhu, Y., Keller, D. and Lu, H. (2000) MDM2 inhibits p300-mediated p53 acetylation and activation by forming a ternary complex with the two proteins. Proc. Natl. Acad. Sci. USA 97, 12547–12552.
[16] Joazeiro, C.A. and Weissman, A.M. (2000) RING finger proteins: mediators of ubiquitin ligase activity. Cell 102, 549–552.
[17] Fang, S., Jensen, J.P., Ludwig, R.L., Vousden, K.H. and Weissman, A.M. (2000) Mdm2 is a RING finger-dependent ubiquitin protein ligase for itself and p53. J. Biol. Chem. 275, 8945–8951.
[18] Honda, R. and Yasuda, H. (2000) Activity of MDM2, a ubiquitin ligase, toward p53 or itself is dependent on the RING finger domain of the ligase. Oncogene 19, 1473–1476.
[19] Honda, R., Tanaka, H. and Yasuda, H. (1997) Oncoprotein MDM2 is a ubiquitin ligase E3 for tumor suppressor p53. FEBS Lett. 420, 25–27.
[20] Tanimura, S., Ohtsuka, S., Mitsui, K., Shirouzu, K., Yoshimura, A. and Ohtsubo, M. (1999) MDM2 interacts with MDMX through their RING finger domains. FEBS Lett. 447, 5–9.
[21] Sharp, D.A., Kratowicz, S.A., Sank, M.J. and George, D.L. (1999) Stabilization of the MDM2 oncoprotein by interaction with the structurally related MDMX protein. J. Biol. Chem. 274, 38189–38196.
[22] Stad, R., Little, N.A., Xirodimas, D.P., Frenk, R., van der Eb, A.J., Lane, D.P., Saville, M.K. and Jochemsen, A.G. (2001) Mdmx stabilizes p53 and Mdm2 via two distinct mechanisms. EMBO Rep. 2, 1029–1034.
[23] Singh, R.K., Iyappan, S. and Scheffner, M. (2007) Hetero-oligomerization with MdmX rescues the ubiquitin/Nedd8 ligase activity of RING finger mutants of Mdm2. J. Biol. Chem. 282, 10901–10907.
[24] Uldrijan, S., Pannekoek, W.J. and Vousden, K.H. (2007) An essential function of the extreme C-terminus of MDM2 can be provided by MDMX. Embo J. 26, 102–112.
[25] Poyurovsky, M.V., Priest, C., Kentsis, A., Borden, K.L., Pan, Z.Q., Pavletich, N. and Prives, C. (2007) The Mdm2 RING domain C-terminus is required for supramolecular assembly and ubiquitin ligase activity. Embo J. 26, 90–101.
[26] Carter, S., Bischof, O., Dejean, A. and Vousden, K.H. (2007) C-terminal modifications regulate MDM2 dissociation and nuclear export of p53. Nat. Cell Biol. 9, 428–435.
[27] Okamoto, K., Kashima, K., Pereg, Y., Ishida, M., Yamazaki, S., Nota, A., Teunisse, A., Migliorini, D., Kitabayashi, I., Marine, J.C., Prives, C., Shiloh, Y., Jochemsen, A.G. and Taya, Y. (2005) DNA damage-induced phosphorylation of MdmX at serine 367 activates p53 by targeting MdmX for Mdm2-dependent degradation. Mol. Cell Biol. 25, 9608–9620.
[28] de Graaf, P., Little, N.A., Ramos, Y.F., Meulmeester, E., Letteboer, S.J. and Jochemsen, A.G. (2003) Hdmx protein stability is regulated by the ubiquitin ligase activity of Mdm2. J. Biol. Chem. 278, 38315–38324.
[29] Li, M., Brooks, C.L., Wu-Baer, F., Chen, D., Baer, R. and Gu, W. (2003) Mono- versus polyubiquitination: differential control of p53 fate by Mdm2. Science 302, 1972–1975.
[30] Ohtsubo, C., Shiokawa, D., Kodama, M., Gaiddon, C., Nakagama, H., Jochemsen, A.G., Taya, Y. and Okamoto, K. (2009) Cytoplasmic tethering is involved in synergistic inhibition of p53 by Mdmx and Mdm2. Cancer Sci.
[31] Gu, J., Nie, L., Wiederschain, D. and Yuan, Z.M. (2001) Identification of p53 sequence elements that are required for MDM2-mediated nuclear export. Mol. Cell Biol. 21, 8533–8546.
[32] Lohrum, M.A., Woods, D.B., Ludwig, R.L., Balint, E. and Vousden, K.H. (2001) C-terminal ubiquitination of p53 contributes to nuclear export. Mol. Cell Biol. 21, 8521–8532.
[33] Shmueli, A. and Oren, M. (2004) Regulation of p53 by Mdm2: fate is in the numbers. Mol. Cell 13, 4–5.
[34] Toledo, F., Krummel, K.A., Lee, C.J., Liu, C.W., Rodewald, L.W., Tang, M. and Wahl, G.M. (2006) A mouse p53 mutant lacking the proline-rich domain rescues Mdm4 deficiency and provides insight into the Mdm2-Mdm4-p53 regulatory network. Cancer Cell 9, 273–285.
[35] Linares, L.K., Hengstermann, A., Ciechanover, A., Muller, S. and Scheffner, M. (2003) HdmX stimulates Hdm2-mediated ubiquitination and degradation of p53. Proc. Natl. Acad. Sci. USA 100, 12009–12014.
[36] Kawai, H., Lopez-Pajares, V., Kim, M.M., Wiederschain, D. and Yuan, Z.M. (2007) RING domain-mediated interaction is a requirement for MDM2's E3 ligase activity. Cancer Res. 67, 6026–6030.
[37] Linke, K., Mace, P.D., Smith, C.A., Vaux, D.L., Silke, J. and Day, C.L. (2008) Structure of the MDM2/MDMX RING domain heterodimer reveals dimerization is required for their ubiquitylation in trans. Cell Death Differ.

Cytoplasmic tethering is involved in synergistic inhibition of p53 by Mdmx and Mdm2

Chihiro Ohtsubo,[1,3] Daisuke Shiokawa,[1,3,6] Masami Kodama,[1,3] Christian Gaiddon,[4] Hitoshi Nakagama,[2] Aart G. Jochemsen,[5] Yoichi Taya[1,3,6,7] and Koji Okamoto[1,2,3,7]

National Cancer Center Research Institute, [1]Radiobiology Division, [2]Early Oncogenesis Research Project, Tokyo, Japan; [3]SORST, Japan Science and Technology Corporation; [4]INSERM U692, Laboratoire de Signalisations Moleculaires et Neurode generescence, Universite de Strasbourg, Faculte de medecine, Strasbourg, France; [5]Department of Molecular and Cell Biology, Leiden University Medical Center, Leiden, The Netherlands

(Received February 17, 2009/Revised March 24, 2009/Accepted March 25, 2009/Online publication April 28, 2009)

The *mdm2* and *mdmx* oncogenes play essential yet nonredundant roles in synergistic inactivation of p53. However, the biochemical mechanism by which Mdmx synergizes with Mdm2 to inhibit p53 function remains obscure. Here we demonstrate that, using nonphosphorylatable mutants of Mdmx, the cooperative inhibition of p53 by Mdmx and Mdm2 was associated with cytoplasmic localization of p53, and with an increase of the interaction of Mdmx to p53 and Mdm2 in the cytoplasm. In addition, the Mdmx mutant cooperates with Mdm2 to induce ubiquitination of p53 at C-terminal lysine residues, and the integrity of the C-terminal lysines was partly required for the cooperative inhibition. The expression of subcellular localization mutants of Mdmx revealed that subcellular localization of Mdmx dictated p53 localization, and that cytoplasmic Mdmx tethered p53 in the cytoplasm and efficiently inhibited p53 activity. RNAi-mediated inhibition of Mdmx or introduction of the nuclear localization mutant of Mdmx reduced cytoplasmic retention of p53 in neuroblastoma cells, in which cytoplasmic sequestration of p53 is involved in its inactivation. Our data indicate that cytoplasmic tethering of p53 mediated by Mdmx contributes to p53 inactivation in some types of cancer cells. (*Cancer Sci* 2009; 100: 1291–1299)

The p53 tumor suppressor plays a central role in the prevention of tumorigenesis.[1,2] p53 exerts its function as a tumor suppressor by transcriptionally activating numerous target genes that are involved in inducing a variety of biological outcomes.[3–5] It is increasingly becoming evident that two related oncogenes, *mdm2* and *mdmx*, play central roles in the regulation of p53 activity.[6,7]

Analyses of knockout mice revealed that *mdmx* and *mdm2* suppress p53 in a nonredundant yet synergistic manner.[8] Mdmx and Mdm2 functionally cooperate to inhibit p53[9,10] and these inhibitors form a heterodimer complex through their RING finger domains.[11,12] Thus, Mdmx and Mdm2 play distinct yet cooperative functions for p53 inactivation, presumably via their physical interaction.

Mdm2 inactivates p53 by targeting it for ubiquitin-mediated proteasomal degradation and by promoting its transport from the nucleus into the cytoplasm,[13] and it is likely that inhibition of p53 by Mdm2 is attributed to these functions. Both functions of Mdm2 require the RING finger domain, which possesses E3 ubiquitin ligase activity. Indeed, Mdm2 functions as an E3 ubiquitin ligase for p53[14] although it has been reported that Mdm2 inhibits p53 via other mechanisms.[15]

In contrast to Mdm2, Mdmx lacks robust activity of an E3 ubiquitin ligase for p53[16] although Mdmx possesses a RING finger domain with high sequence similarity to that of Mdm2. In accordance with its inability to ubiquitinate p53 by itself, Mdmx-dependent inhibition of the transcriptional activity of p53 is independent of p53 degradation.[17] Recently, it was reported that Mdmx can complement the E3 activity of C-terminal mutants of Mdm2, suggesting that Mdmx contributes to p53 suppression in a manner distinct from Mdm2.[18,19]

In the present paper, by using nonphosphorylatable Mdmx mutants that are resistant to degradation by Mdm2, we showed that Mdmx and Mdm2 synergistically induce the cytoplasmic retention of p53 in DNA transfection assays. We demonstrated that cytoplasmic Mdmx, but not nuclear Mdmx, efficiently cooperates with Mdm2 to keep p53 in the cytoplasm and inhibits p53 activity. Further, RNAi-mediated inhibition of Mdmx or introduction of nuclear localization mutants of Mdmx reduced cytoplasmic retention of p53 in neuroblastoma cells. It has been documented that p53 is sequestered in the cytoplasm in some types of cancer, such as neuroblastoma, and the sequestration of p53 is likely to contribute to its inactivation. We will discuss how Mdmx and Mdm2 contribute to cytoplasmic sequestration of p53, and its implication during development of some types of cancer.

Materials and Methods

Cell lines. H1299 and U2OS cells were maintained in Dulbecco's modified Eagle's medium supplemented with 10% fetal calf serum.

Antibodies. Anti-Flag antibody (M2) was purchased from Sigma. Anti-p53 monoclonal antibody (DO-1) was purchased from Calbiochem. Anti-HA antibody was purchased from Roche (F Hoffmam-La Roche Ltd, Basel, Switzerland). Anti-myc-tag antibody (9E10), anti-GFP antibody (B-2), anti-topoisomerase I antibody (C-2), anti-γ tubulin antibody (D-10), and anti-Mdmx antibody (D-19) were purchased from Santa Cruz (Santa Cruz, CA).

DNA transfection. In DNA transfection experiments, 2 μg DNA and 4 μL Lipofectamine 2000 reagent (Invitrogen) were introduced per 2.0×10^5 cells. Transfected cells were then incubated for 20 h before harvesting. In experiments in which the subcellular localization mutants of Mdmx were transfected to determine localization of endogenous p53, Lipofectamine LTX (Invitrogen, Carlsbad, CA) was used instead according to the manufacturer's protocol.

Luciferase assay. Twenty hours after transfection, cells were lysed and luciferase activity was measured using the Dual-Luciferase Assay System (Promega, Madison, WI). Mean values (±SD) from three independent experiments were determined. Basal promoter activity expressed in the absence of HA-p53 was measured and subtracted in each experiment.

Immunostaining. Cells were fixed in 4% paraformaldehyde in PBS for 10 min, washed with 1× PBS, and permeabilized in 100% methanol for 30 min at –20°C. The fixed cells were then used for immunostaining as previously described.[20]

[6]Present address: Cancer Science Institute of Singapore, National University of Singapore, Singapore 117456.
[7]To whom correspondence should be addressed. E-mail: kojokamo@ncc.go.jp; nmiyt@nus.edu.sg

doi: 10.1111/j.1349-7006.2009.01180.x